ELECTROSPUN POLYETHERIMIDE AND POLYBENZIMIDAZOLE FIBERS AND COMPOSITES

A Thesis

by

FATEMA HA-MIM BINTA HAFIZ

Submitted in Partial Fulfillment of the

Requirements for the Degree of

MASTER OF SCIENCE

Major Subject: Chemistry

The University of Texas Rio Grande Valley

December 2021

ELECTROSPUN POLYETHERIMIDE AND POLYBENZIMIDAZOLE FIBERS AND COMPOSITES

A Thesis
by
FATEMA HA-MIM BINTA HAFIZ

COMMITTEE MEMBERS

Dr. Javier Macossay-Torres
Chair of Committee

Dr. Debasish Bandyopadhyay
Committee Member

Dr. M. Jasim Uddin
Committee Member

Dr. Wei Lin
Committee Member

Dr. Jose Bonilla-Cruz
Committee Member

December 2021

ABSTRACT

Hafiz, Fatema Ha-mim Binta., Electrospun polyetherimide and polybenzimidazole fibers and composites. Master of Science (MS), December, 2021, 65 pp., 26 tables, 33 figures, references, 21 titles.

In this study, polymer micro and nanocomposite fibers with PBI and PEI as polymer, and exfoliated graphite and nitroxide-functionalized graphene oxides have been prepared. Electrospinning has been chosen as a fiber processing technique. This work describes the electrospinning process of the mentioned polymer fibers and composite fibers followed by their characterization by XRD, ATR, SEM, TGA, DSC, and tensile testing.

DEDICATION

The completion of my master's would not have been possible without the love and support of my family. They wholeheartedly inspired, motivated, and supported me to accomplish this degree. Thank you for your love and patience.

ACKNOWLEDGMENTS

I would first like to thank my thesis advisor Dr. Javier Macossay-Torres. I would like to thank him for keeping me in place emotionally, whenever I ran into a trouble spot or had a question about my research or writing. He consistently allowed this paper to be my own work but steered me in the right direction whenever he thought I needed it.

I would also like to acknowledge Dr. Debasish Bandyopadhyay, Dr. Jose Bonilla-Cruz, Dr. Wei Lin and Dr. M. Jasim Uddin, for being the committee members of this thesis, and I am gratefully indebted to their very valuable inputs on this thesis. I also express my gratitude to Tom Embunk for helping me with the SEM. I appreciate the assistance and willingness of helping from Dr. Jose Bonilla-Cruz and his team from Centro de Investigacion en Materials Advanzado, S. C (CIMAV) (Unidad Monterrey).

Finally, I must express my very profound gratitude to my lab-mates Diego, Dominic, Kingsley and Mayra for providing me with unfailing support and continuous encouragement. Thanks to the University of Texas Rio Grande Valley and the department of Chemistry for giving me this opportunity to have an excellent research experience.

TABLE OF CONTENTS

Page

LIST OF TABLES

Page

LIST OF FIGURES

Page

CHAPTER I

INTRODUCTION

Nanocomposite science opens a wide platform for designing new and versatile nanomaterials suitable for numerous different applications with adjustable properties and functionality. It is usually defined as multiphase solid materials where at least one phase has one dimension in nanometers range. Technically nanocomposites are different from conventional composite materials as it offers the idea of building material blocks in nanometer dimensions and developing flexible new materials with improved physical properties due to high surface to volume ratio of reinforcing phase. The success of effective high-performance composites depends on the dispersion of the filler materials into the matrix material. A wide range of natural and synthetic polymers can be used as matrix materials for versatile application due to unique interaction between polymer and nanoparticles and it introduces the possibility to improve, and desired property combination of nanomaterial incorporated with polymeric network. It makes the polymer nanocomposites significant among nanocomposites.

Recently a lot of initiatives have been taken to produce carbon-based nanocomposites that have a huge number of potential applications for having large defined surface area, excellent electrical and thermal conductivity, and high mechanical properties. Nanocomposites containing the combination of carbon nanomaterials and polymer introduce new nanocomposites with advanced and improved functional and structural and functional properties for wide range of applications. [6, 2]

Graphene is one of the most widely studied carbon-based structures as because it has a very good tensile strength, electron mobility and thermal conductivity. Nanoscale uniform dispersion of graphene in a polymeric matrix makes a significant impact on polymer performance.[6] Polyetherimide (PEI) is a special type of polyimide (PI)that is developed to overcome the challenge (thermal stability, mechanical strength) associated with polyimide. It is a relatively new type of polyimide polymer material that contains an excellent collection of attributes like superior thermal stability, high mechanical strength, stiffness, good electrical properties, high flame resistance and broad chemical resistance.[4] Along with PEI another high-performance polymer PBI is also used for this study. In recent years it is considered one of the most attracted high-performance polymers of great deal of interest due to its outstanding heat stability and chemical resistance with decomposition temperature of more than 500 ^{0}C. Another interesting property of PBI is its glass transition temperature about 425 ^{0}C with no melting point with high heat deflection temperature. PBI also have low level of ionic impurities and outgas (ex H_20).[11]

For the progression of this study rather than using any conventional methods, electrospinning has been chosen as a fiber processing technique for PEI and PBI nanofibers. In recent years resulting fibers and this technique both have been widely used and adopted for numerous purposes like polymer preparation, composite and structured fibers required diameter from nano to micrometer for both academic and industrial interest. This fiber processing technique opens the large possibility of having fibers with high specific surface area and controllable structure of fibers with low density and high porosity.

CHAPTER II

LITERATURE REVIEW

The very first reference of nanocomposite related study was found around 1950. The first reported literature of nanocomposite was reported by Blumstein in 1961. Around early 1980 Toyota's Central Research and Development Laboratories started working with polymer-layered silicate-clay mineral composites (Acquarulo & O'Neil). [1]

Preparation of graphene from graphite created more opportunity for graphene based nano composite. The synthesis of graphite oxide (GO) from oxidation of graphite was first reported by Brodie in 1859 (potassium chlorate and nitric acid was used for the oxidation). [2] After that various chemical and thermal methods were used to exfoliate GO. [2] Stanchovich et al. reported synthesis of GO from aqueous solution suspension and hydrazine with the help of ultrasonication.[2] Wang et al. prepared exfoliation of GO using hydroquinone and hydroiodic acid. MacAllister et al. used thermal method for exfoliation of GO.[2] Kranbuehl et Al. used 1000 ^{0}C temperature and generated carbon dioxide which exaggerated pressure on graphite sheets and resulted exfoliation. [2] Grafting is another common method used for the exfoliation of GO. Xu et.[2] al used grafting method; they used esterification for the exfoliation of GO filler.[2] Yazmin et al. synthesized nitroxide-funtionalized graphene oxide (GOFT) from GO with the help of oxoammonium salt. [3]

Literatures reported various incorporation methods for polymer-graphene nanocomposite. Polarization of polymer using amphiphilic substance was reported by Kato et al.[2] Valdes et al.

Reported ethylene acid co-polymerization technique.[2] Schniepp et al. used maleic anhydride as a bridge element between polymer and exfoliated graphene. Mittal et al. used melt mixing method for exfoliated polymer – graphene nanocomposite.[2] Kim et al reported polyethylene functionalization and blending method for polyethylene graphene nanocomposite. [2]Liang et al. reported solution mixing method for polyurethane and isocyanate modified graphene nanocomposite.[2] Kuila et al worked-on epoxy graphene oxide nanocomposite. Li et al reported polyurethane epoxy graphene nanocomposite using in situ synthesis method.[2] Scognamilo et al developed TPU nanocomposites with graphene within situ polymerization.[2] Appel et al prepared PU nanocomposite with TRGO graphite oxide.[2]

Wilson et al. reported in situ intercalation polymerization for polymer graphene generation. Kalaitzidou et al. used melt intercalation method for polymer – graphene nanocomposite.

Chinu and Huang used solution mixing method for the preparation of PI –graphene nanocomposite to improve the electrical conductivity. [4]Mittal et al. reported preparation of polyamide nanocomposite with GO containing improved mechanical properties.[2] Heo and Chang fabricated PI nanocomposite using functionalized graphene and observed enhanced thermal conductivity.[4]

Liu et al. prepared electro spun PI graphene composite nanofiber. Ramakrishnan et al. reported PI GO nanofiber composite.[4] Wang et al. fabricated electrospun PI go composite nanofiber. All this graphene based electrospun polyimide nanofiber obtained improved mechanical, thermal and electrical properties.[4]

Electrospinning, the fiber processing technique was first reported by Renekar group in 1990. Khan et al. reported electrospun polycaprolactone nanofiber.[4] Nakata et al. developed

electrospun polyether sulfone nanofiber for heat resistant high performance air filter.[4] Cesar et al. worked on the characterization of electrospun Nylon 6 nanofiber containing GOFT. [8]Javier et al reported about SEM, TGA and FTIR characterization of electrospun Polystyrene multiwalled carbon nanotube composite nanofiber.[9] In another paper Macossay et al. reported about mechanical and biocompatibility studies of electrospun Tecoflex composite nanober containing multiwalled carbon nanotubes.[7] Electrospinning process of polymethyl methacrylate nanofiber and its composite nanofiber with vapor grown carbon was explained by Macossay et al.[10] Electrospinning of polyamide functionalized by GO and the influence of the crystal structure was reported by Javier et al.[11]

Zhang et al explained preparation of electrospun polyimide nanofiber. The first report about the mechanical property of electrospun polyimide nanofiber was published on 2008.[4] Hou et al developed measuring method for tensile strength and stain of electrospun PI nanofiber.4 They reported about excellent strength and toughness of PI nanofibers. Miao et al. first reported their study about the role of electrospun PI nanofiber as lithium-ion battery separator. [4]Takemori and Kawakami discussed about the possibility of using electrospun polymer nanofiber as fuel ceel proton exchange membrane.[4] They developed polymer electrolyte membrane based on electrospun PI sulfonated exchange membrane.[4] Zhang et al. reported about the filtration performance of electrospun PI. They observed the removal of pollutant particles at high temperature.[4]

Electrospinning of PBI was first made by Kim and Renekar. The first development work on PBI was reported in 1960.[5]

Very few reports have been found on the development of electrospun PEI and PBI composite nanofiber where graphene-based particles were used as reinforcing material. The

objective of this study was to observe the effect of different percentages of different graphene-based filler materials on the microstructural, Mechanical and thermal properties of PEI and PBI. The objectives were

- To synthesize different graphene derivates reinforce material
- To prepare polymer solutions with optimized concentration for electrospinning
- To electrospin PBI and PEI using electrospinning technique.
- To disperse the reinforcing materials in the polymer matrix by using high-energy sonication.
- To obtain polymers/reinforcing materials nanofibers from electrospinning.
- To characterize the nanofibers using SEM, TGA, FTIR, Tensile Testing.

CHAPTER III

SAMPLE DEVELOPMENT

Introduction

The primary purpose of this study was to electrospin Polyetherimide (PEI) and Polybenzimidazole (PBI) using the optimize condition foe electrospinning. Another purpose of this study was to determine the effect of different concentrations of dispersed reinforce material in two different polymer matrix and their resulted electrospun nanofiber.

Two different high-performance polymers were reinforced with different concentrations of three graphene based reinforce materials expanded graphite (EG), nitroxide-functionalized graphene oxide (GOFT) and nitroxide-functionalized graphene oxide from expanded graphite GOFT (EG**)**. Reinforcing material especially graphene based reinforcing materials have significance influence regarding the thermal, mechanical, electronic and optical properties of the polymer nanofibers.

Improvement of polymer nanofiber properties mostly depends on the uniform dispersion of the reinforcing material within the polymer matrix other factors like solvent properties, solution and reinforce concentration, polymer properties structure and orientation polymer are also responsible for the potential produce of continuous aligned nanofiber. To select appropriate method to be best implemented for this investigation prior research have been carried out

regarding several parameters like processing conditions, solution properties and ambient conditions.

There are five different preparation methods for polymeric-based graphene nanocomposite which are solution casting technique, melt blending technique, in-situ polymerization, electrodeposition and electrospinning. To produce fine composite nanofiber with diameter from nano to micrometer range electrospinning method can be used.[5]

In this study electrospinning has been chosen as a fiber formation technique for this investigation since this method has the potential to produce highly oriented continuous nanofibers with controlled diameter and morphology.

Material selection

Polymer solution preparation

Polybenzimidazole (PBI) and Polyetherimide (PEI) both are well known for their high performance with excellent physical and chemical stability. 26% PBI obtained from Performance products, Inc. diluted upto14% using Dimethylacetamide (DMAc) (N, N-Dimethylacetamide 99% pure (DMAc) were obtained from Acros Organics).[14] On the other hand, Polyetherimide (PEI) was obtained from Sigma-Aldrich Corporation. Polyetherimide (PEI) was obtained from Sigma-Aldrich Corporation. Tetrahydrofuran 99.8% Extra Dry (THF), was obtained from (Acros Organics). 15% PEI solution was prepared using solvents DMAc/THF in 50:50 ratio (with respect of the volume of the two solvents). For example, 1.5 g of PEI was dissolved in 10 ml solvent of DMAc/THF (5 ml of DMAc and 5 ml of THF). The polymer and the solvents were weighed out and combined, then vortexed for about 5 minutes, and left in a warm water bath for 2-4 hours at 40-50°C. After that the solution was left on a bench top shaker (Tekmar electronic

VXR at 150 RPM) until the polymer was completely dissolved. 14% PBI solution was prepares using solvent DMAc, both of them were weighed out and combined, then vortexed for about 5 minutes and equilibrated for about one day on a bench top shaker (Tekmar electronic VXR at 200 RPM).

Figure 1: Polymer solutions of PBI and PEI

Reinforcing materials preparation

Three types Three types of graphene based reinforcing materials expanded graphite (EG), nitroxide-functionalizad graphene oxide from graphite flex (GOFT) and nitroxide-functionalizad graphene oxide from expanded graphite [GOFT(EG)] were prepared for this study.

Preparation of expanded graphite (EG)

Expanded graphite (EG) was prepared by mixing Graphite, potassium permanganate, and concentrated sulfuric acid in 5:1:30 weight ratio. For example1g of graphite, 0.200g of potassium permanganate and 6g of sulfuric acid was mixed. After mixing, this mixture was heated at 50^{o}C for 30 minutes with continuous high-speed stirring. After that the product was filtered using vacuum filtration method where silk was used as filter. Filtrated product kept in over for complete evaporation of water. That was a commercial microwave oven (Sharp Carousel R-209HK) and the volume of the product increased after microwave irradiation .[16]

Figure 2: Treated graphite before and after microwave irradiation

Preparation of GOFT and GOFT (EG)

GOFT and GOFT (EG) have been prepared following same procedure but the starting material was different. At the first step of synthesis for GOFT graphene oxide (GO) was prepared from pure graphite. For the preparation of GOFT (EG), graphene oxide (GO) was prepared from EG. In both syntheses improved modified Hummer's method was followed using Sodium nitrate, Potassium permanganate, Hydrogen peroxide, Sulfuric acid and Hydrochloric acid. In second step Oxoammonium salt (Br- Tempo) was prepared by mixing Bromine, Tempo and anhydrous carbon tetra chloride. Soxhlet extraction was utilized for purification and filtration of the prepared product. At the last step GO was mixed with triethylamine and dimethylformamide solution and the total mixture was sonicated at 150 W for 30 minutes. After finishing sonication, this dispersion was mixed drop wise with a solution of dimethylformamide and Br-Tempo. Then the entire mixture was placed in a N_2 atmosphere at 2 ^oC for 4 hours to confirm the exfoliation and functionalization. (17, 3)

Dispersion of reinforcing materials

The dispersions of polymer- reinforcing material were prepared by adding reinforcing

Figure 3: Prepared GO and GOFT

materials in polymer solution at 0.1, 0.5 and 1% wt. with respect to the polymer and then sonicated with a 500-watt ultrasonic processor (Sonics Vibra-cell model VCX 500) at 20 kHz with 20% amplitude The ultrasonic wand was placed inside the vials and the wand was kept in touch with the solution. The solution was placed in a beaker packed in ice bath to avoid excessive heat generation and to minimize solution evaporation. The solution was sonicated for 1h at 20% amplitude and the sonication process was paused in every 20 minutes to check the ice level.

Electrospinning process

To electrospin polymer and polymer-composite fibers, polymer and dispersion solutions were transferred into a 10 mL glass syringe with 18-gauge stainless steel needle. Air bubbles were removed, and the needle was tested for clogs. A static electrospinning setup was used for all electrospinning. The syringe was placed on a syringe infusion pump (KD Scientific KDS-200 dual). The needle tip was connected with the positive terminal. A round copper plate attached to a wooden block was used as collector and the negative terminal was connected with this.[14] The flow rate and amount of solution were controlled using the infusion pump. For PBI the flow rate was 0.1ml/hr. The distance between the needle tip and collector plate was 35 cm and the applied voltage was +25 V and -8 V. For PEI the applied voltage was +17.5 V and -10 V. For PEI the flow rate was 3ml/hr. and the distance between the needle tip and collector plate was 30 cm.

Figure 4: Electrospun PBI and PEI nanofibers.

CHAPTER III

XRD ANALYSIS

Introduction

XRD is one of the most commonly used methods to investigate the structural features of nanocomposites due to its ease and availability. XRD is a versatile, non-destructive characterization technique that can offer thorough information about chemical composition. It is also one of the most convenient techniques towards the characterization of polymer-based nanocomposite.[17]

Instrument

For XRD characterization power X-ray diffraction (XRD, Panalytical Empyream) was used with Bragg-Brentano geometry (where $80^{o} \geq \theta \geq 5^{o}$, 10.16 s, 0.0167113 s).[3]

Method

Crystal atoms scatter incident X-rays, primarily through interaction with the atoms' electrons. This phenomenon is known as elastic scattering; the electron is known as the scatterer. A regular array of scatterers produces a regular array of spherical waves. In the majority of directions, these waves cancel each other out through destructive interference, however, they add constructively in a few specific directions, as determined by Bragg's law: $2dsin\theta = n\lambda$,

Where *d* is the spacing between diffracting planes, θ is the incident angle, *n* is an integer, and λ is the beam wavelength. The specific directions appear as spots on the diffraction pattern called reflections. Consequently, X-ray diffraction patterns result from electromagnetic waves impinging on a regular array of scatterers.[17,18]

Results and Discussion

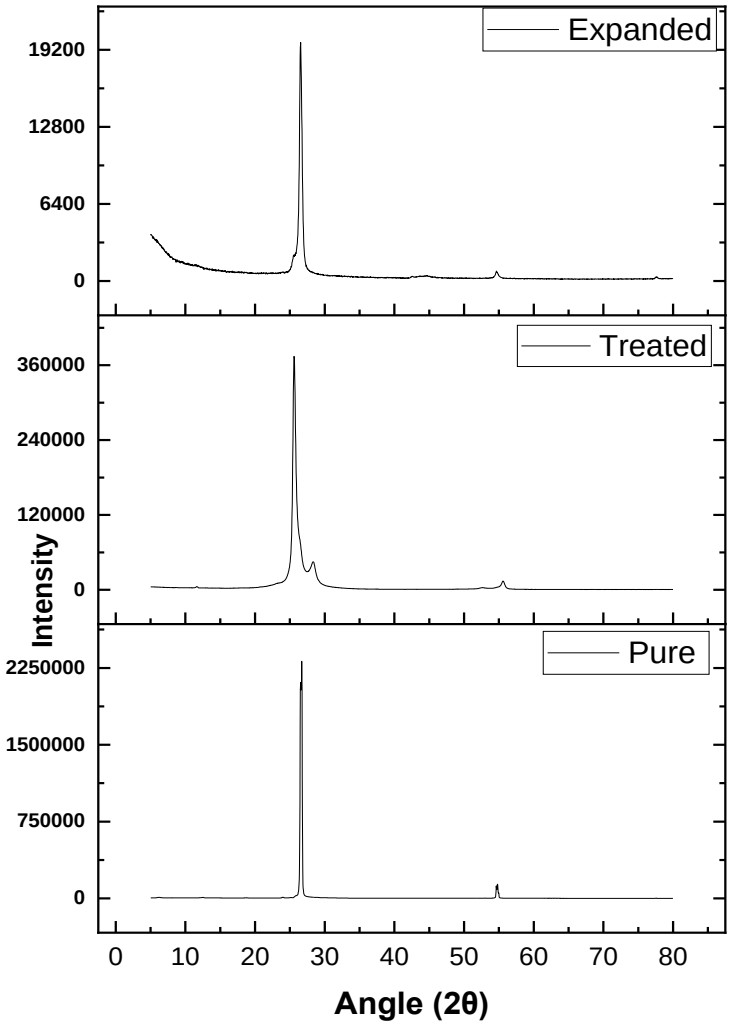

Figure 5: XRD spectra of pure graphite, treated graphite and expanded graphite.

Figure 5 represent change occurred after treating the graphite. In a pure graphite XRD spectrum, the prominent peak appeared at 27 degree. But, after that pure graphite was treated

with acid and permanganate a shoulder peak appeared at 30 degrees. This appearance of the shoulder peak shift is indication of intercalation of sulphuric acid. Moreover, another peak observed at 55 degrees in pure graphite has shifted to 57 degree. The peak shifting occurred due to the intercalation of sulfuric acid. After microwave irradiation, the shoulder peak disappeared and another peak moved to the 55 degree. Intensity value decreased for expanded graphite and this decreased value indicated the exfoliation.

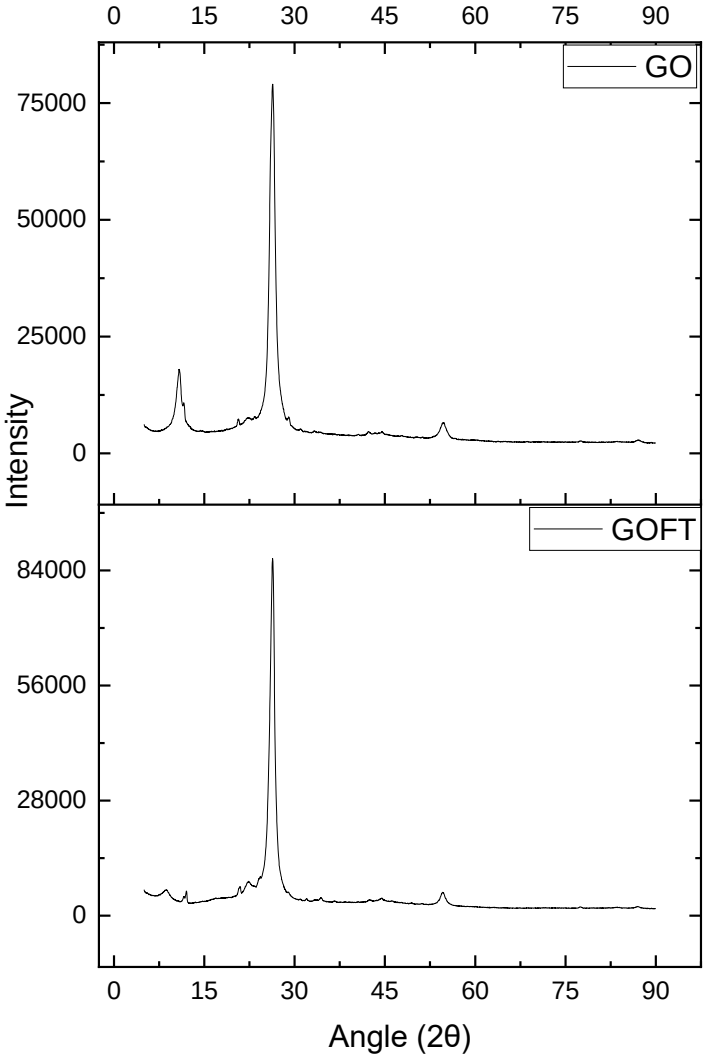

Figure 6: XRD spectra of GO and GOFT

Figure 6 represents XRD spectra from GO synthesized from Hummer's method and XRD spectra of GOFT. In both spectra there was a peak at 27 degree which indicated the highly organized layer structure of graphite. In GO spectra the peak around 10 degree confirmed the oxidation of graphite. In GOFT spectra the peak at 10 degree disappeared due to complete oxidation of graphite and exfoliation. From the XRD spectra of GO and GOFT (EG) in figure 3 it was observed that both of the XRD spectra has the characteristic graphite peak at around 27 degree. The peak at the 10 degree for GO disappeared in GOFT (EG) confirming the complete oxidation and exfoliation.

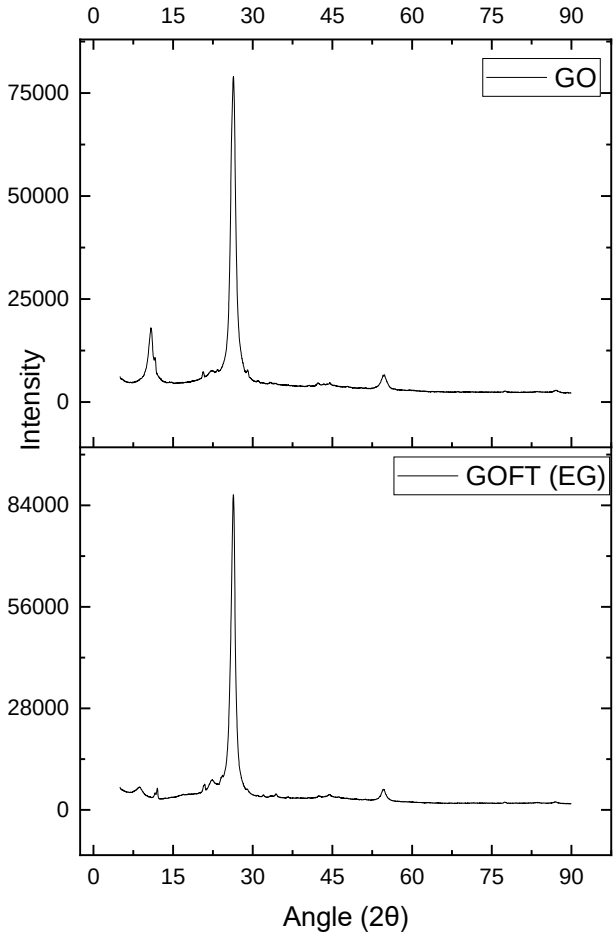

Figure 7: XRD spectra of GO and GOFT (EG)

CHAPTER IV

MICROSTRUCTURAL ANALYSIS

Introduction

SEM is used in this study as a surface analysis technique; it is a type of electron microscope used here for a direct surface-related study of reinforcing materials and nanofibers. Generally, utilizes a beam of focused electrons of relatively low energy as an electron probe that is scanned in a regular manner over the specimen. The action of the electron beam stimulates the emission of high-energy backscattered electrons and low-energy secondary electrons from the surface of the specimen. It images the sample surface by scanning it with a high-energy beam of electrons in a raster scan pattern. The primary electron beam, which is produced under a high vacuum, is scanned across the surface of a specimen. When the electrons strike the specimen, a variation of the signal produces an image of the surface, or its elemental composition together with energy dispersive X-rays.[23]

Instrument

A Denton Vacuum Desk II self-contained sputter and etch unit and a Leo 435 VP scanning electron-microscope were utilized to produce micrographs of the electrospun nanofibers and reinforcing materials.

Method

The nanofiber samples received an ultrathin coating of palladium, an electrically conducting alloy, by low vacuum sputter coating. This was done in order to prevent static electric charge during the electron irradiation and to improve the contrast and resolution by improving the signal. The argon pressure in the chamber was set at about 6-7 psi. The samples were loaded on a pedestal holder and the sputter deposition was begun when the chamber was at 30 millitorr or less. The timer was set to a desired deposition time. The samples were coated in two 30 second consecutive cycles at 45 mA. When the deposition time elapsed, the sputtering device was turned off. The samples were placed on a silicon wafer and inserted into the sample chamber where micrographs were taken at various magnifications. Micrographs were obtained from the microscope operating at an accelerating voltage of 3.9 KV and saved for comparison. Nanofibers were observed on a monitor at various magnifications.[25]

Results and Discussion

To observe the morphologies of reinforcing materials and nanofiber SEM was used. Magnification for this set of micrographs was 5 KX. From the SEM image of the pure graphite, treated graphite and expanded graphene (EG) (figure 3.1), it was observed that the layer present in the pure graphite was irregular, compact with rough surface nature, where treated graphite clear, smooth surface with distinguish layer. For EG no particular rough layer with loose sponge like appearance could be seen.

SEM images of GO, GOFT, GO (EG) and GOFT (EG) (from figure 3.2) confirm the expansion and functionalization with well-defined and interlinked porous network of graphene

sheets, magnification was 10 KX. The surface nature of GO and GO (EG) was completely different from the surface nature of GOFT and GOFT (EG).

The micrographs from figure 3.1 represent the change of surface nature while preparing the reinforcing material EG and the micrographs from Figure 3.3 represent the change in the surface nature from GO to GOFT and from GO (EG) to GOFT (EG).

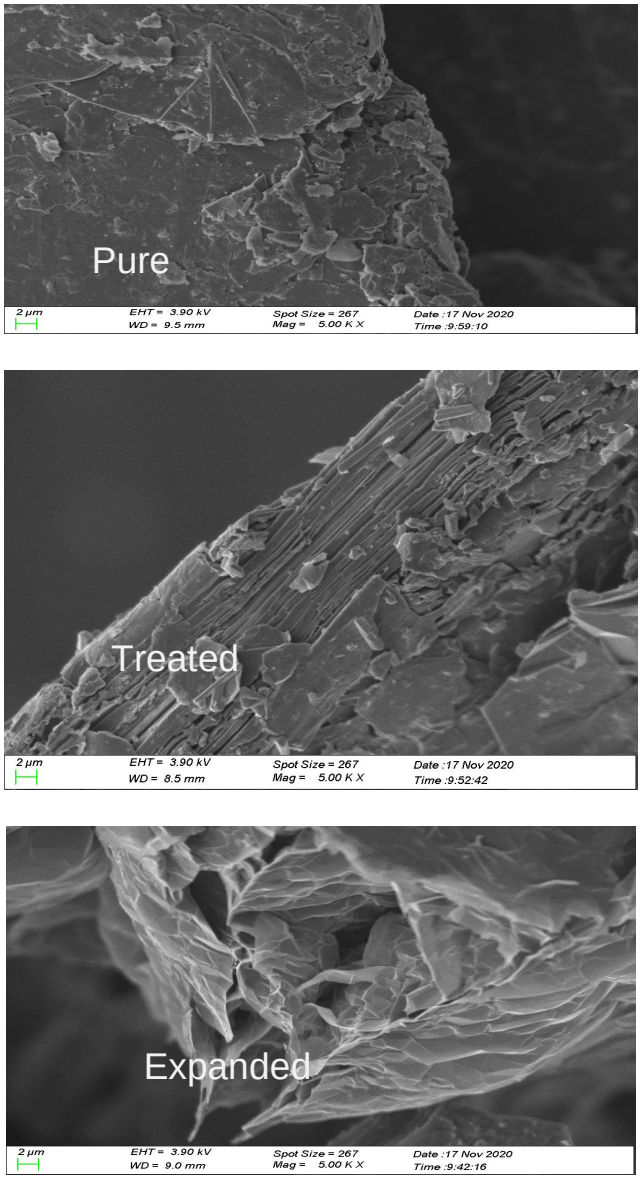

Figure 8: SEM images of Pure treated and expanded graphite.

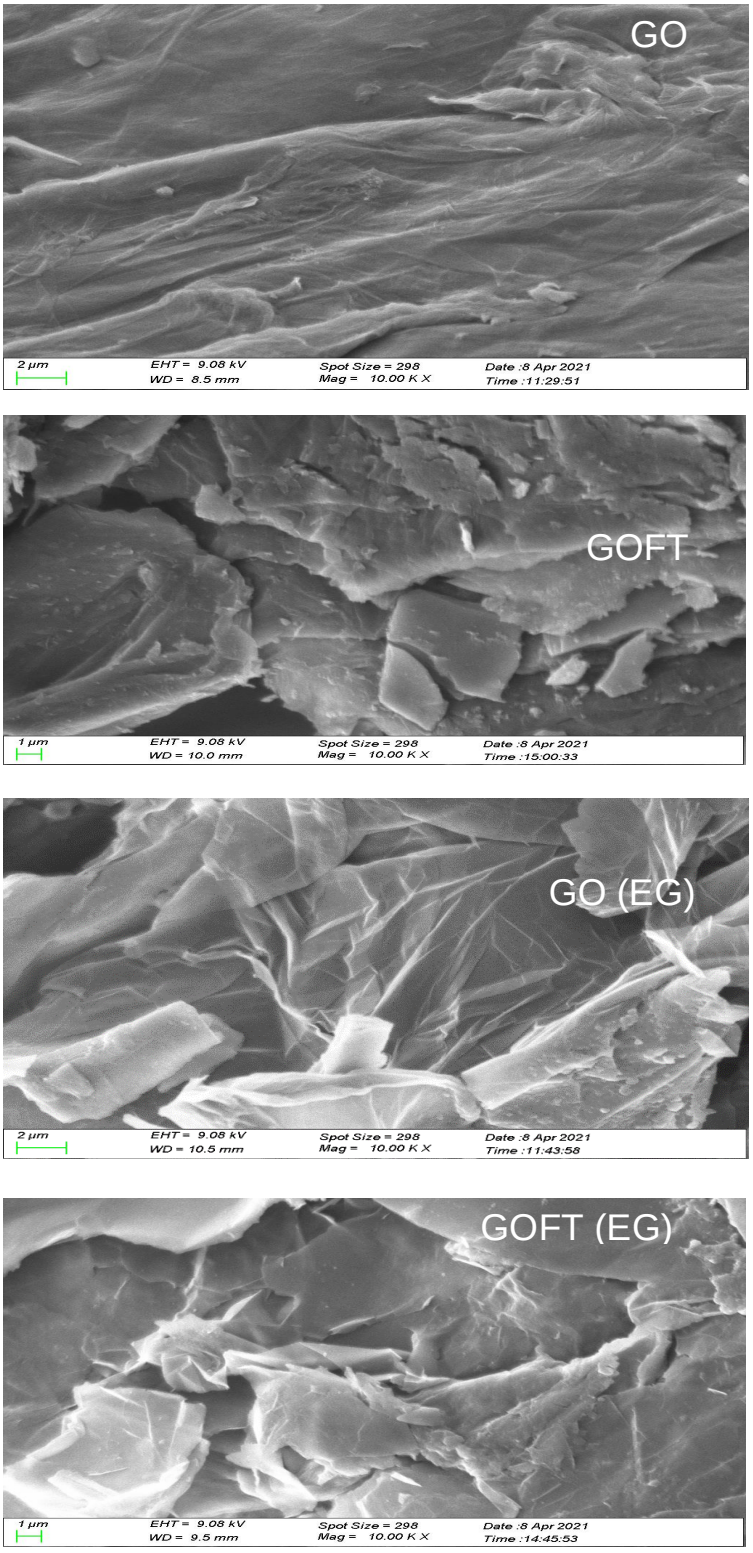

Figure 9: SEM images of GO, GO (EG), GOFT and GOFT (EG).

SEM of fibers and composites

SEM image of PBI had some solvent droplet with average diameter 274 nm. PBI nanofibers with EG (reinforcing material) experienced significant decrease in the fiber diameter. The average fiber diameter of PBI nanofibers with 0.1%,0.5%,1.0% (with respect to polymer mass) EG was mentioned in the following table1. Nanofibers with EG have no beads. From the table it was observed that 0.5% had the lowest fiber diameter.

Table 1: Fiber diameter of PBI nanofiber with different percentage of EG

Sample	Fiber diameter (nanometers)
PBI	274 ± 54
PBI+0.1% EG	226± 32
PBI+0.5% EG	210± 54
PBI+1% EG	243± 39

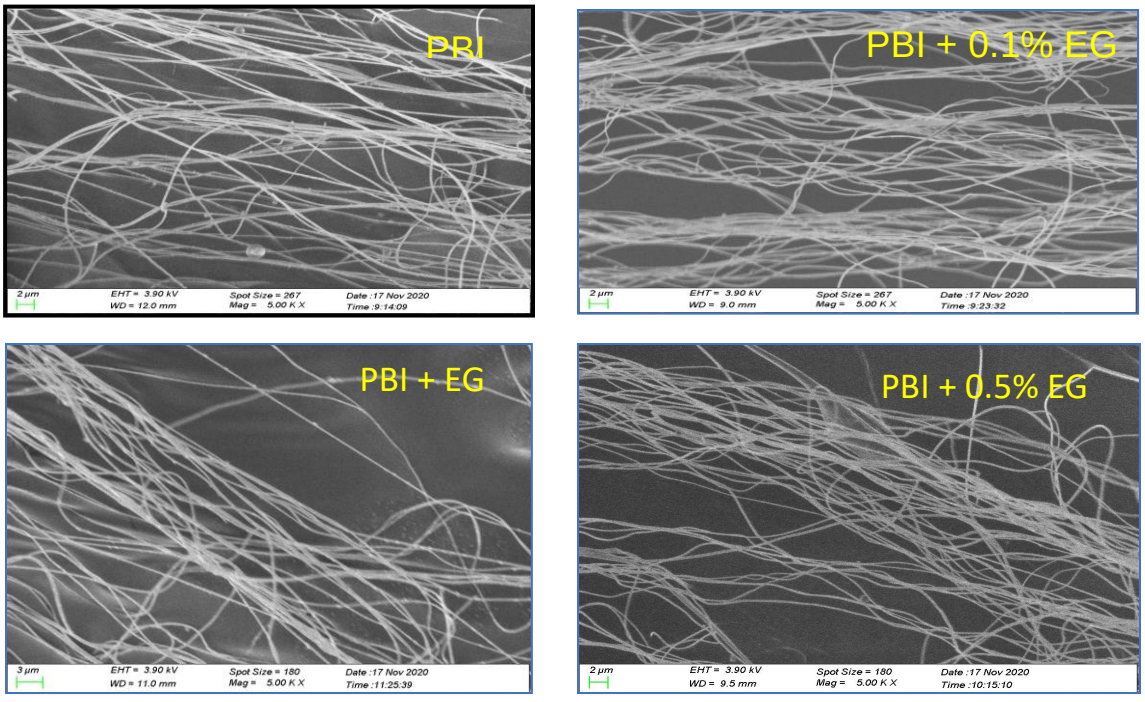

Figure 10: SEM image of PBI, PBI+0.1% EG, PBI+0.5% EG, PBI+1.0% EG

The next set of micrographs (figure 10) were from the samples PBI with 0.1%, 0.5% and 1.0% (with respect of the polymer mass) of GOFT and magnification was 5 KX. The average diameter of the nanofibers experienced more decrease and became narrower with the introduction of GOFT. The average fiber diameter of PBI nanofiber with 0.1%, 0.5%, 1.0% GOFT is given below in the table 2. Nanofibers with 0.5% and 1.0% GOFT had beads. PBI nanofiber with 1% GOFT had the lowest fiber diameter.

Table 2: Fiber diameter of PBI nanofiber with different percentages of GOFT

Sample	Fiber diameter (nanometers)
PBI	274 ± 54
PBI+0.1%GOFT	183± 33
PBI+0.5%GOFT	185± 40
PBI+1%GOFT	196± 43

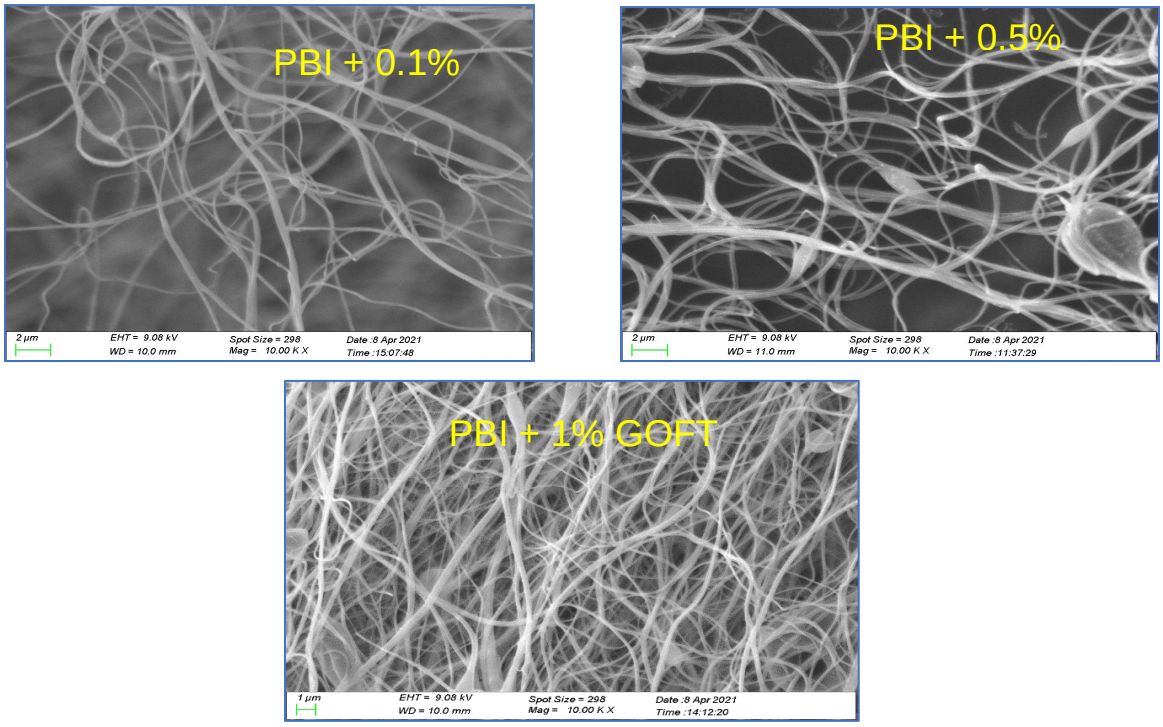

Figure 11: SEM image of PBI + 0.1% GOFT, PBI + 0.5% GOFT, PBI + 1.0% GOFT

Another set of micrographs was taken for the samples PBI with GOFT (EG). The presence of GOFT (EG) produced the narrowest PBI nanofiber among these three reinforcing materials. For 0.1%, 0.5%, 1.0% GOFT (EG) the average fiber diameter is mentioned in following table. Nanofiber with 0.1% GOFT (EG) had some beads. Following the table data, it was observed that fiber diameter increased with the increased percentage of GOFT (EG) and 0.1% GOFT (EG) offered the narrowest PBI nanofiber.

Table 3: Fiber diameter of PBI nanofiber with different percentages of GOFT (EG)

Sample	Fiber diameter (nanometers)
PBI	274± 54
PBI+GOFT(EG) 0.1%	137± 30
PBI+GOFT(EG) 0.5%	167± 48
PBI+GOFT (EG) 1%	264 ±36

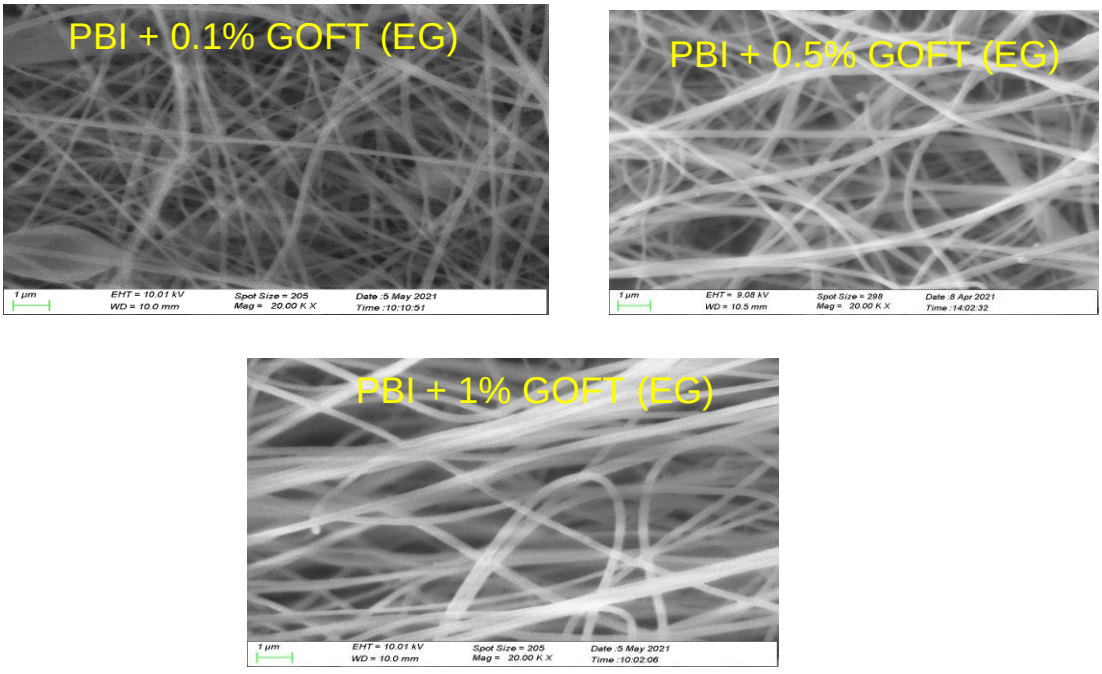

Figure 12: SEM image of PBI + 0.1% GOFT (EG), PBI + 0.5% GOFT (EG), PBI + 1.0% GOFT (EG)

On the other hand PEI nanofibers with reinforce material came up with different results. The micrograph of PEI nanofibers was beads-free and average fiber diameter was 2029 nm. With the reinforcing material EG there was a significant increase in the nanofiber diameter, Table 4 contains the average fiber diameter for 0.1%, 0.5%, 1.0% (with respect to the polymer mass) GOFT (EG) respectively.

Table 4: Fiber diameter of PEI nanofiber with different percentages of EG

Sample	Fiber diameter (nanometers)
PEI	2029± 306
PEI+0.1% EG	2699± 287
PEI+0.5% EG	2861± 492
PEI+1% EG	2373 ± 28

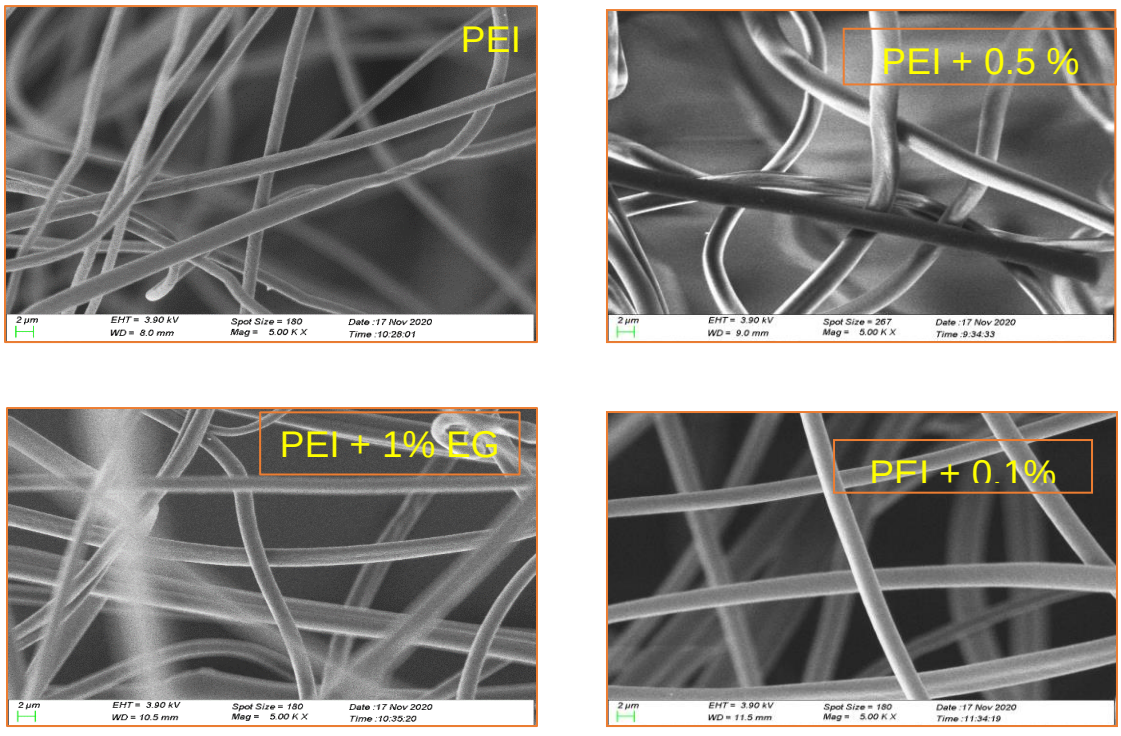

Figure 13: SEM image of PEI, PEI+0.1% EG, PEI+0.5% EG, PEI+1.0% EG

The micrographs of PEI with GOFT appeared with a significant decrease with the increase of reinforcing material GOFT. The average fiber diameter mentioned 0.1%, 0.5%, 1.0% GOFT in the table 5. PEI nanofiber with 0.1% GOFT had larger diameter than PEI nanofiber without GOFT and PEI nanofiber with 0.5 % GOFT experienced drastic decrease but PEI nanofiber with 1.0 % GOFT obtained the narrowest fiber diameter.

Table 5: Fiber diameter of PEI nanofiber with different percentages of GOFT

Sample	Fiber diameter (nanometers)
PEI	2029± 306
PEI+0.1%GOFT	2289± 47
PEI+0.5%GOFT	1241± 382
PEI+1%GOFT	123 ±19

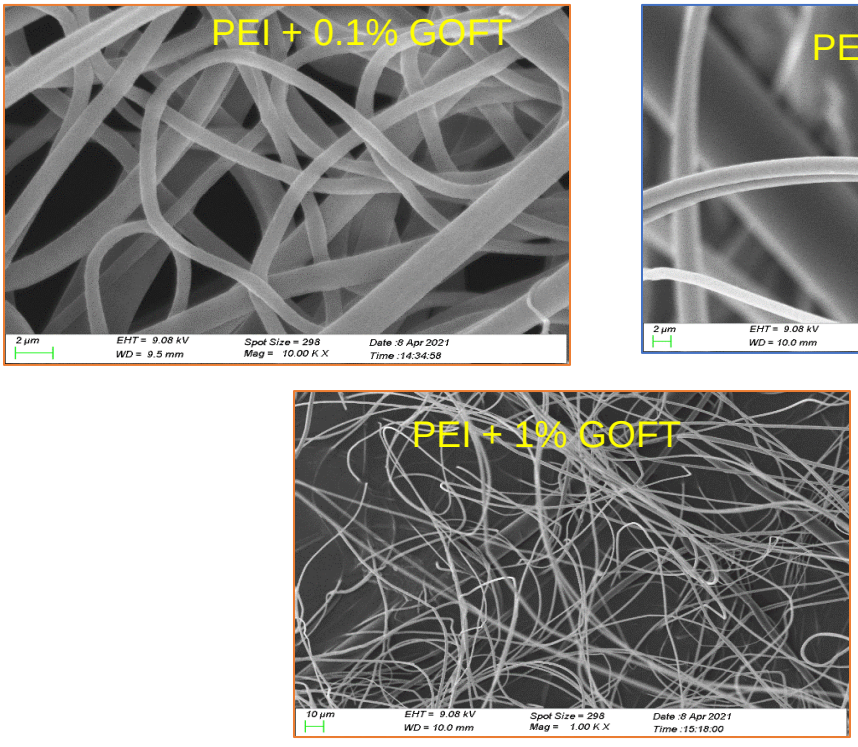

Figure 14: SEM image of PEI + 0.1% GOFT, PEI + 0.5% GOFT, PEI + 1.0% GOFT

The next set of micrographs was from PEI with different concentrations of GOFT (EG). GOFT (EG) also promoted a significant decrease in fiber diameter. The average fiber diameter was for 0.1%, 0.5%, 1.0% (with respect to the polymer mass) GOFT (EG) was provided in the table 6. PEI nanofiber with 0.1% filler contained larger diameter and fiber diameter decreased with the increased amount of GOFT (EG).

Table 6: Fiber diameter of PEI nanofiber with different percentages of GOFT (EG)

Sample	Fiber diameter (nanometers)
PEI	2029± 306
PEI+GOFT(EG) 0.1%	2994± 167
PEI+GOFT(EG) 0.5%	1805±157
PEI+GOFT (EG) 1%	481±51

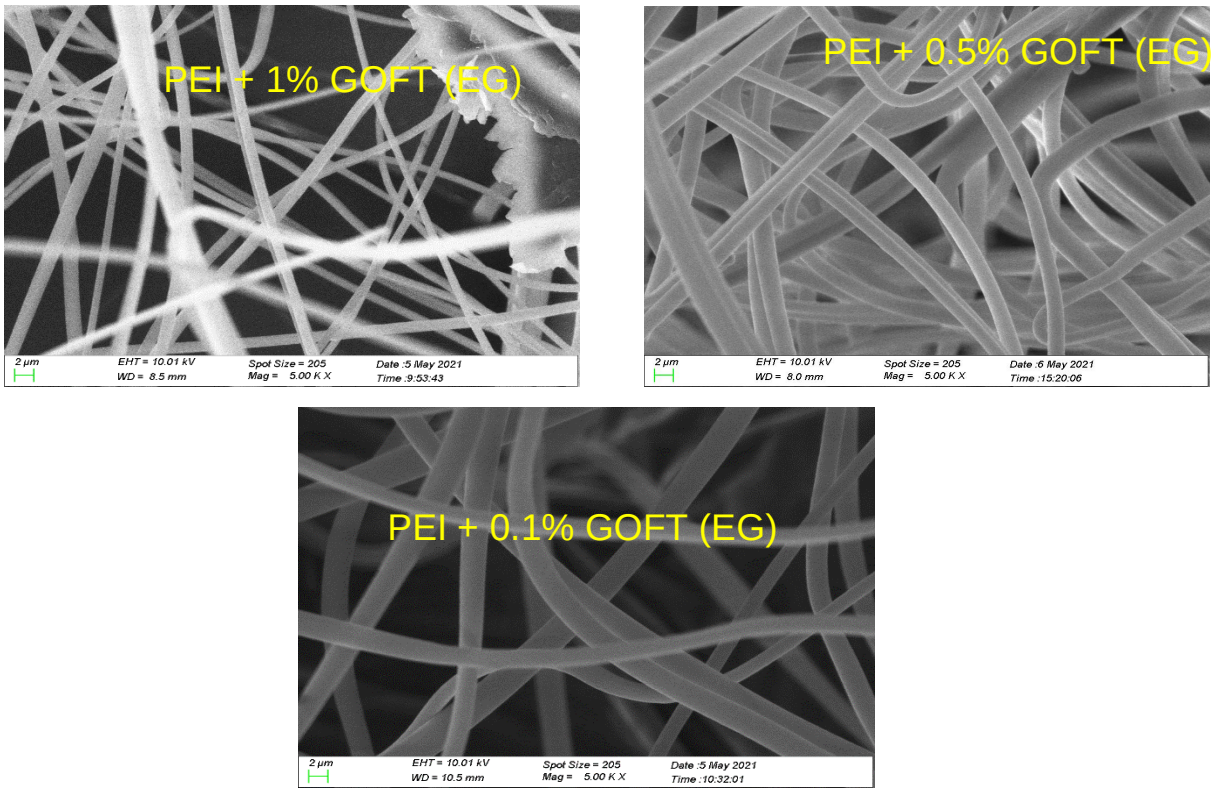

Figure 15: SEM image of PEI + 0.1% GOFT (EG), PEI + 0.5% GOFT (EG), PEI + 1.0% GOFT (EG)

All the PEI nanofiber with EG, GOFT and GOFT (EG) had the bead free appearance. PEI nanofiber with all reinforcing material follow the similar pattern, with the increasing percentage of reinforcing material, fiber diameter decreases.

The significant decrease of nanofiber diameter may happen due to low resistivity of polymer system. Addition of graphene-based reinforcing material may encourage resistivity decrease, which on the other hand cause increase in conductivity and charge density and can promote elongation of fiber. This elongation of fiber during fiber formation may decrease the diameter.[7] But with the increasing amount of reinforcing material it is difficult to hold the preferential alignment which disturbs the surface tension distribution that is why an increase in fiber diameter could be observed with the increase of reinforcing material (the fiber diameter of PBI with 1% EG, GOFT and GOFT (EG) was experiencing a slight increase than 0.5% and 0.1%).[7]

For PEI nanofiber with EG as reinforcing material may come up with uneven dispersion of filler within polymer matrix and perturb the physical interaction which affect the surface tension property and increase the diameter of the nanofibers.

Appearance of beads or droplet like structure in polymer nanofiber may result from rapid solvent evaporation during electrospinning process.[25]

CHAPTER V

SPECTROSCOPIC ANALYSIS

Introduction

After Fourier transform infrared spectroscopy – attenuated total reflectance (FTIR–ATR) gives information about particular functional groups, and chemical structure of polymer materials. Shifts in the transmission frequency and changes in relative band intensities provide information about changes in the chemical structure or changes in the environment around the sample. That is why, FTIR–ATR spectroscopy is generally used for determining the outcome of the surface chemistry of chemical or physical modifications. The spectroscopic technique provided help to determine the chemical nature of the polymer composite surface. Considering the nature of the composite, relevant information regarding the surface chemistry can be collected to understand the component composition of the surface.[26]

Instrument

Infrared Spectroscopy was done with a Bruker ALPHA Platinum ATR single reflection diamond ATR and OPUS software with the resolution set to 4 cm^{-1}, scans set to 256, and background scans set to 256. The frequency range used was 4000-400 cm^{-1}.[25]

Method

An ATR-FTIR spectroscopic technique is used to characterize the polymer and polymer nanocomposite because it is simple to handle, and it has almost universal acceptability. An ATR-FTIR generally measures the changes in reflected IR beam when the beam comes into contact with a sample. An IR beam is directed on a dense crystal material with a high refractive index with a particular angle. The internal reflectance creates an evanescent wave that extends beyond the surface of the crystal into the sample contacted with the crystal.

In the IR spectrum regions where the sample absorbs energy, the evanescent wave will be attenuated. The attenuated beam comes back to the crystal, then exits through the opposite end of the crystal and is directed to the detector in the IR spectrometer. The detector records the attenuated IR beam as an interferogram signal, which is used to generate an IR spectrum.[25]

Results and discussion

For the confirmation of the formation of Polyetherimide (PEI) and Polybenzimidazole (PBI) polymer nanofibers FTIR-ATR analysis was observed. Fig 16 and Fig 19 represents the electrospun PBI and PEI nanofibers respectively.

For PBI at 3190 cm-1 single bond stretch absorption peak was found for secondary amine and N-H peak was found at 1611 cm^{-1}. For aromatic C=C bond, there was a peak at 1440 cm^{-1} in the double bond region and at 1290 cm^{-1} there was a peak for C-N stretching of aromatic amine. In the fingerprint region, the peak at 803 cm^{-1} corresponding to C-H bending of 1,3,4 (asymmetric) tri-substituted benzene and the peak at 609 cm^{-1} was for rocking of N-H bond. The peak at 606cm^{-1} and 458 cm^{-1} corresponds to the rocking of C-H bonds and meta substituted benzene.

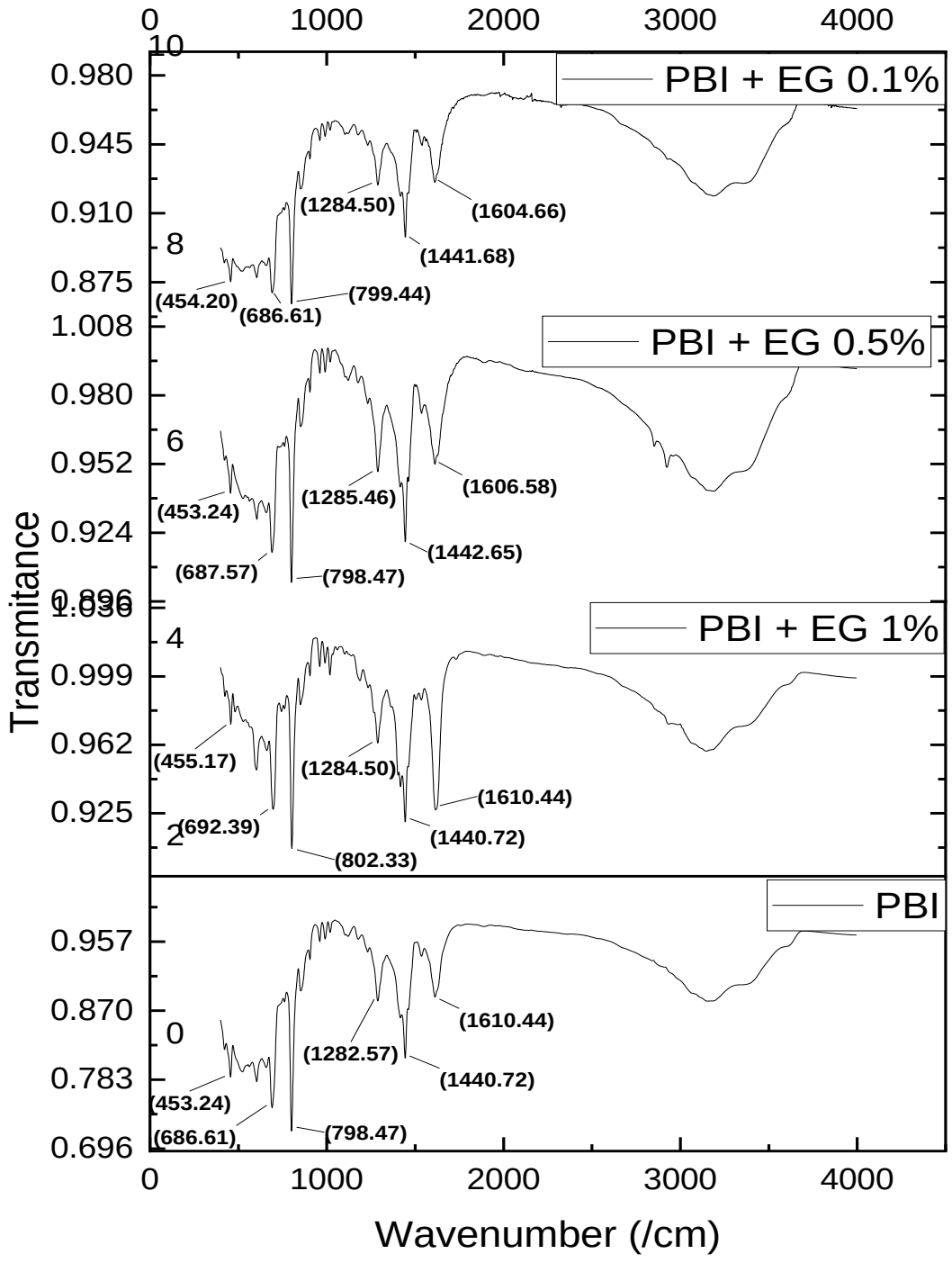

Figure 16: FTIR spectra of PBI nanofiber and PBI nanofiber with different percentages of EG

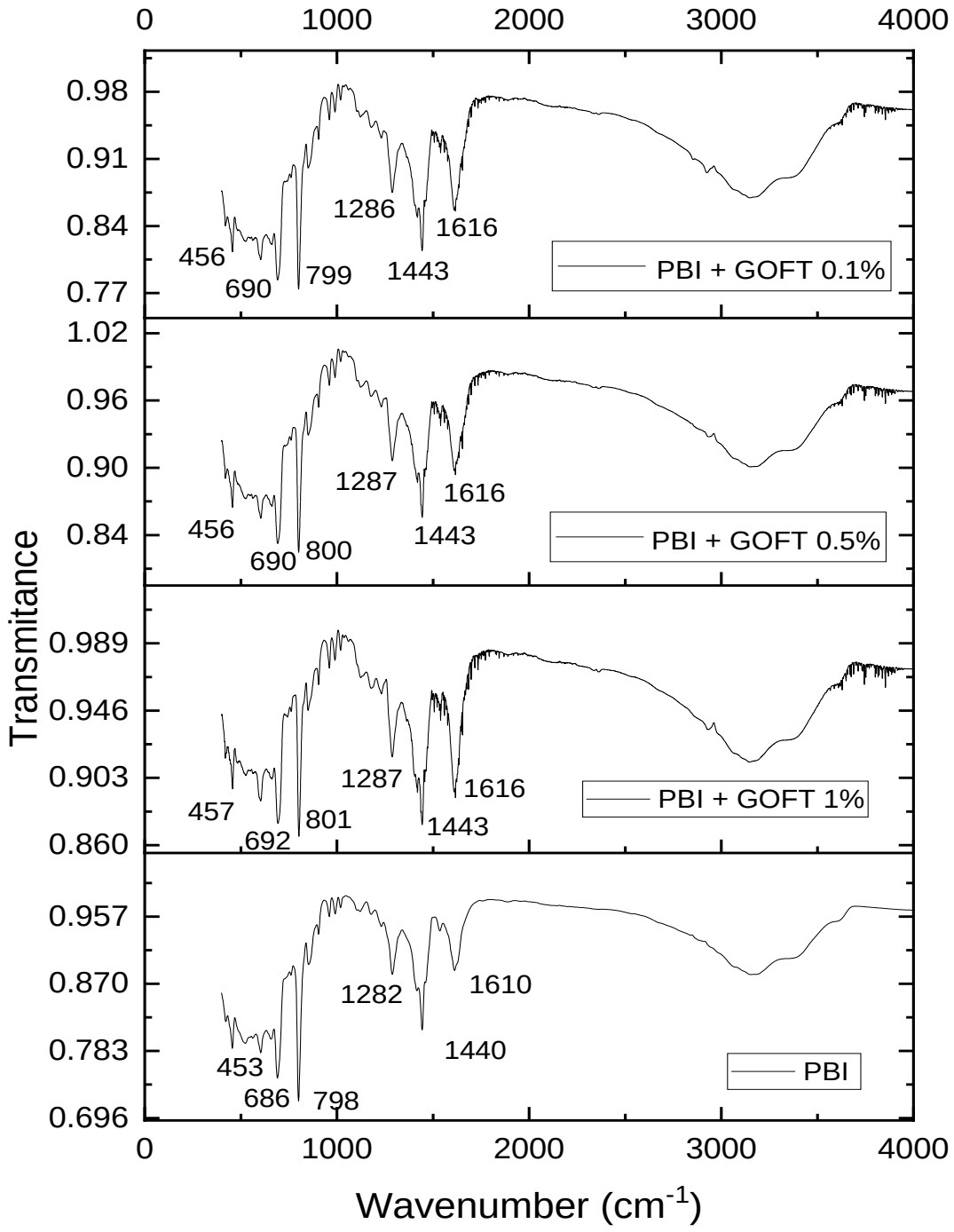

Figure 17: FTIR spectra of PBI nanofiber and PBI nanofiber with different percentages of GOFT

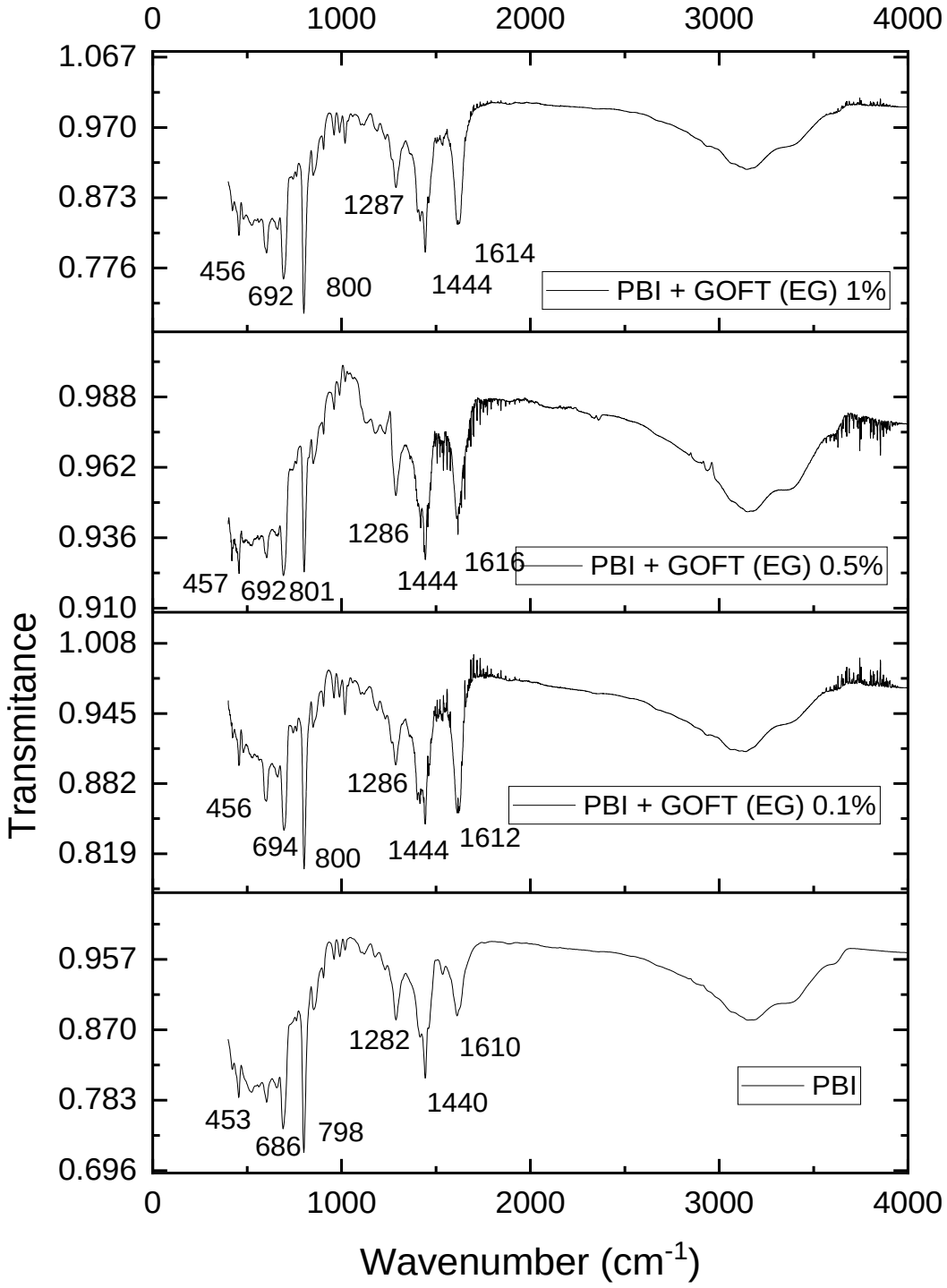

Figure 18: FTIR spectra of PBI nanofiber and PBI nanofiber with different percentage of GOFT (EG)

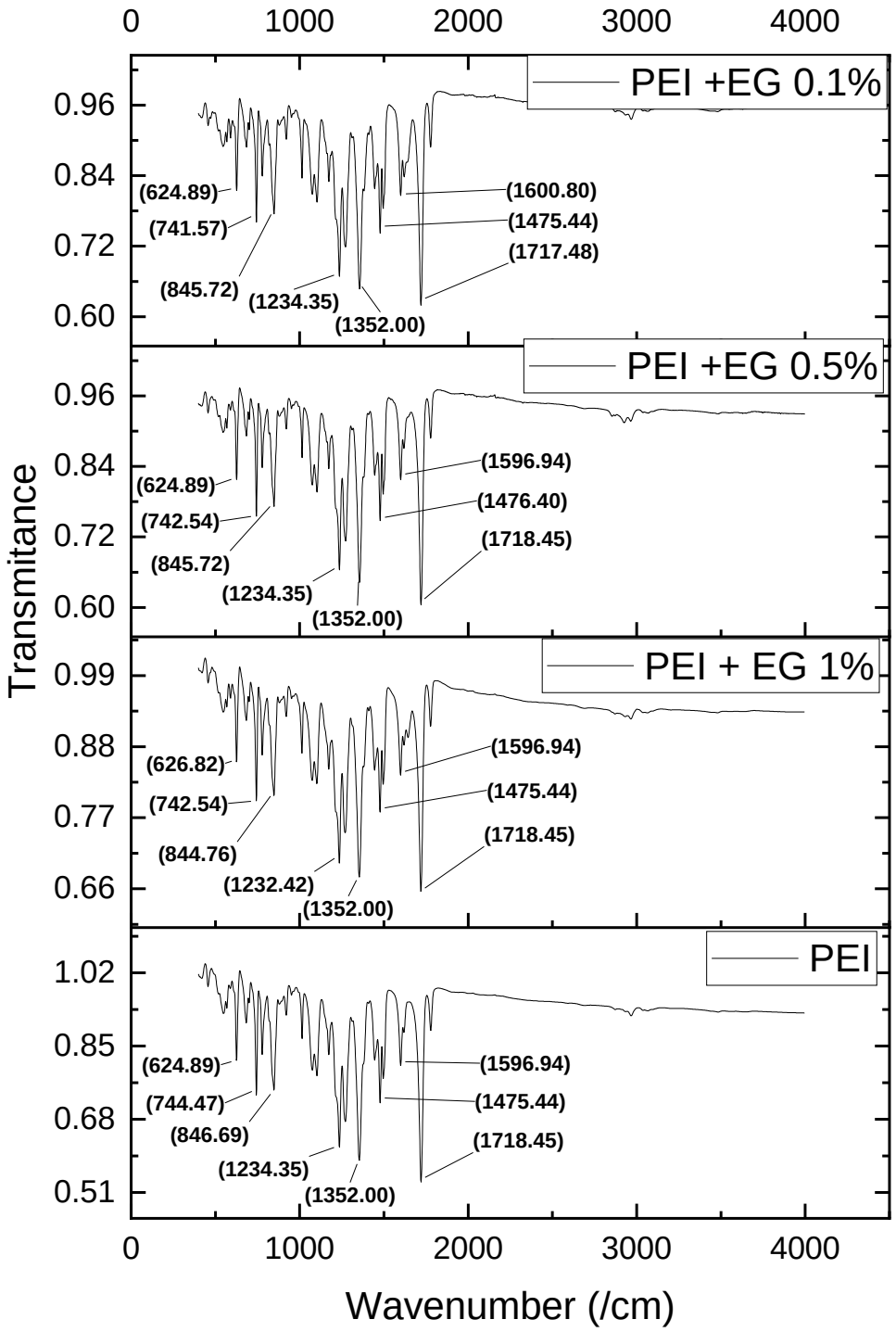

Figure 19: FTIR spectra of PEI nanofiber and PEI nanofiber with different percentage of EG

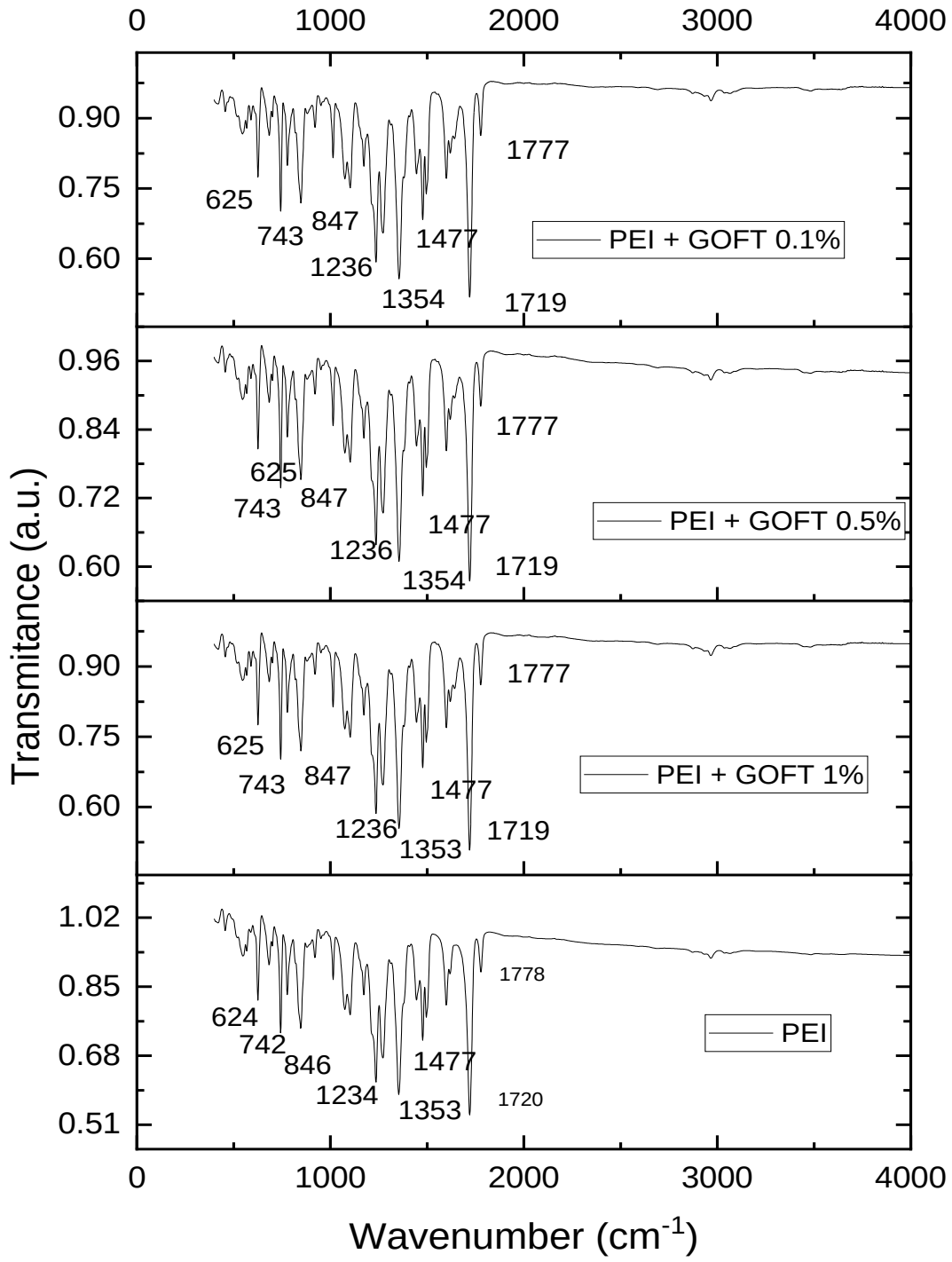

Figure 20: FTIR spectra of PEI nanofiber and PEI nanofiber with different percentage of GOFT

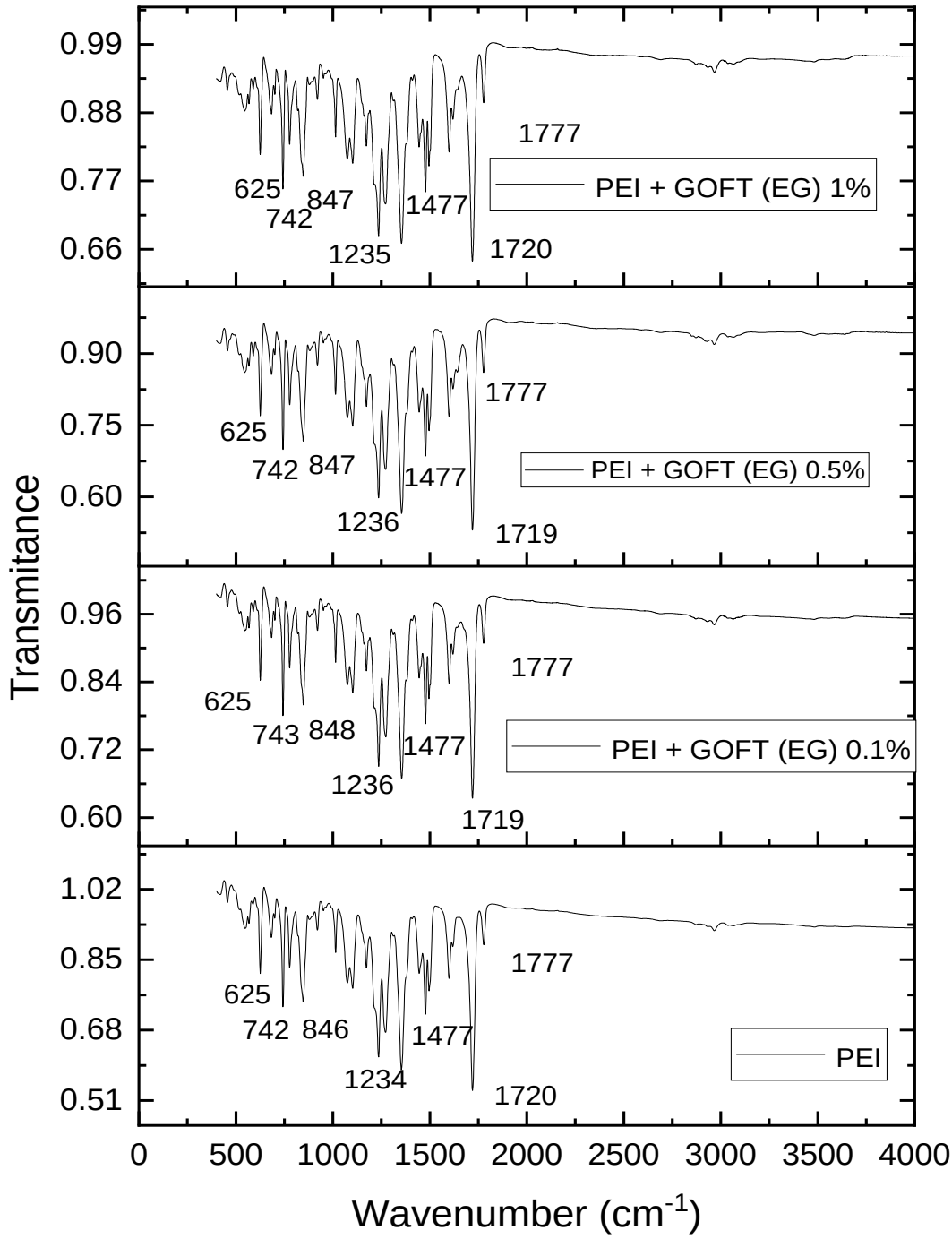

Figure 21: FTIR spectra of PEI nanofiber and PEI nanofiber with different percentage of GOFT (EG)

For PEI, the peak at 1780 cm^{-1} and 1720 cm^{-1} corresponds to the characteristic peak of imide group, typical asymmetric and symmetric imide carbonyl stretch. For C-N stretching and bending there was peak at 1355cm^{-1} and 743 cm^{-1} respectively. The peak at the 1234 cm^{-1} related with aromatic ether C-O-C.

The identification of the characteristic peak was confirmed by comparing the sample spectra to a reference spectrum. The peak positions of electrospun polymer nanofibers were slightly different from the theoretical peak positions.

For PEI nanofibers with different percentage of expanded (EG) graphite have all the characteristic peaks and the position of all those peaks was observed to be remained same. This observation represents the possibility of formation of weak interfacial interaction between PEI and EG. PEI nanofibers with different percentage of GOFT and GOFT (EG) exhibits similar characteristic peaks and almost all the peak maintained the same position as pristine PEI.

For PBI nanofibers with different concentrations of EG almost no shift of peak position was observed compared with the peak position of PBI itself. Similar spectroscopic observation also observed for PBI nanofibers with different concentrations of GOFT and GOFT (EG), there was no change or minimal change in the position of all the characteristic peaks.

A non-covalent approach with π-π reformation along with hydrogen bonding and electrostatic force may be the reason for having similar output from both polymer nanofibers with graphene derivate reinforcing materials.[6] By comparing the minimal significant change in peak position of PBI and PEI nanofibers with all three-reinforcing material EG, GOFT, GOFT (EG) it was observed that PBI nanofibers had more significant change in peak position shifting. The increased number of carbon and hydrogen bonding may create an interaction for electronegative nitrogen and result in more significant peak shift than PEI.

CHAPTER VI

MECHANICAL STRENGTH ANALYSIS

Introduction

Mechanical strength of polymer nanofiber using the tensile testing method is one of the most fundamental types of mechanical testing methods. Usually in this type of testing method tensile force applies on the testing material and the material response as stress and this measured stress introduces a way of determination of the strength of material within elongation capability. Tensile testing machine usually has a test frame consisting load cell, testing software. Using tensile tests, we were able to obtain values for the maximum load (N) of the material, tensile stress (MPa) and tensile strain (mm/mm) as well as Young's modulus (MPa). The maximum load helps determine the maximum force a material can withstand. The tensile stress is the maximum amount of stress a material can withstand before it breaks. Tensile strain refers to the degree of deformation of a polymer when stress is applied. The Young's modulus is a ratio of the stress acting on the material to the strain produced and therefore measures the resistance of the stress acting on the material to the strain produced and therefore measures the resistance of a material to deform when a load is applied.[14]

Instrument

The tensile strength and percent elongation of the electrospun fiber were evaluated using an INSTRON® tensile tester 5943 with a 25 N maximum load cell under a crosshead speed of 10 mm/min.

Method

The samples utilized for mechanical characterization were cut using a die that shaped the electrospun materials into a "dog-bone" shape. The die-cut the samples with a 2.75 mm width at their narrowest point and a gauge length of 7.5 mm. A Fractional Digital Caliper was used to measure the thickness of each dog-bone shaped sample. A minimum of 6 samples were used to test the tensile behavior of the polymer and the average values were recorded. Data from tensile strength was then replotted using origin software.[14]

Results and discussion

Table 7 demonstrates the numerical values. From the numerical value and the figure, it was observed that the PBI nanofiber has low tensile strain and tensile stress is higher than strain and elongation did happen. The Young's modulus of PBI nanofiber was about 93 MPa. According to the result PBI is strong with high resistivity of deformation and tensile strength.

Table 7: Tensile strength tests for PBI

Data	N Total	Mean	Standard Deviation
Maximum Load (N)	7	0.143	0.077

Tensile Stress (MPa)	7	5.010	0.322
Young's Modulus (MPa)	7	93.009	93.863
Tensile Strain (mm/mm)	7	0.091	0.035

The addition of reinforcing material EG , there was a sharp decrease in Young's modulus, PBI nanofiber with 0.1 % EG has Young's modulus about 9.9 MPa with higher tensile strain and low tensile stress. With the increase in percentage, PBI nanofiber with 0.5% EG experience lower young modulus, tensile stress and tensile strain than 0.1%. PBI nanofiber with 1% EG exhibited a slight improvement in the young modulus, tensile stress and tensile strain value.

All these observations indicate that with the addition of EG PBI nanofibers become flexible with low resistivity of deformation.

Table 8: Tensile strength tests for PBI with 0.1% EG

Data	N Total	Mean	Standard Deviation
Maximum Load (N)	7	0.198	0.100
Tensile Stress (MPa)	7	0.921	0.412
Young's Modulus (MPa)	7	9.920	4.267
Tensile Strain (mm/mm)	7	0.209	0.096

Table 9: Tensile strength tests for PBI with 0.5% EG

Data	N Total	Mean	Standard Deviation
Maximum Load (N)	6	0.177	0.096
Tensile Stress (MPa)	6	0.878	0.490
Young's Modulus (MPa)	6	6.555	3.114
Tensile Strain (mm/mm)	6	0.197	0.046

Table 10: Tensile strength tests for PBI with 1.0% EG

Data	N Total	Mean	Standard Deviation
Maximum Load (N)	7	0.441	0.186
Tensile Stress (MPa)	7	1.542	0.632
Young's Modulus (MPa)	7	7.925	3.364
Tensile Strain (mm/mm)	7	0.327	0.113

The next tables 11,12,13 demonstrated the tensile behavior of PBI nanofibers with 0.1%, 0.5% and 1.0% (with respect to the polymer mass) GOFT. Again with the addition of GOFT, PBI nanofibers experienced decrease in Young's modulus and tensile stress value and an increase in tensile strain value. For nanofiber with 0.1% GOFT Young's modulus dropped up to 59.9 MPa

and the tensile stress was almost similar as PBI nanofiber with no reinforced material but tensile

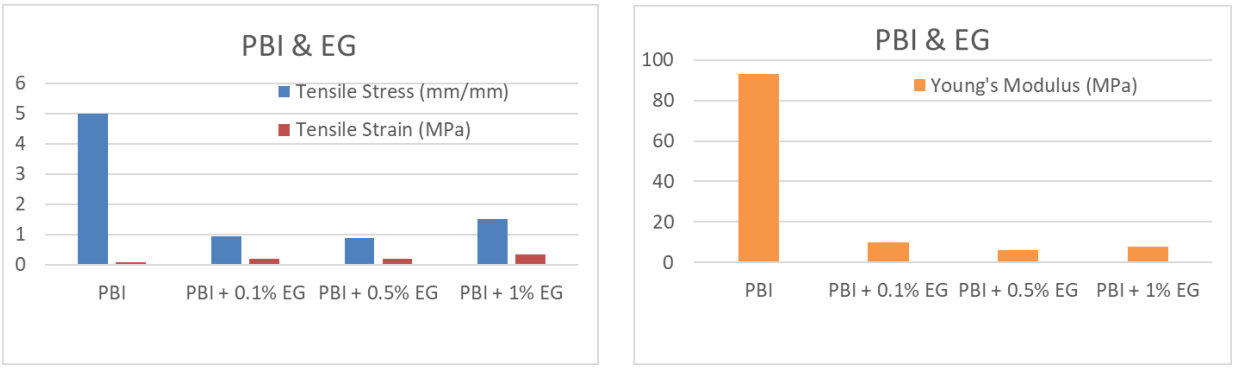

Figure 22: Tensile parameters for PBI nanofibers with EG

strain increase up to 0.17. With the increasing percentage of GOFT, PBI nanofiber with 0.5% GOFT there was an increase in Young's modulus value, it was up to 74 MPa but the tensile stress and tensile strain value decreased. With highest percentage of GOFT PBI nanofiber experienced the lowest Young's modulus and tensile stress among all the three percentages of GOFT; on the other hand it occupied the highest tensile strain value. Observing all these tensile testing output, it can be concluded that the addition of GOFT decreases the deformation rigidity and increases the flexibility of PBI nanofiber. But PBI nanofibers with GOFT are more rigid and strong than PBI nanofibers with EG.

Table 11: Tensile strength tests for PBI with 0.1% GOFT

Data	N Total	Mean	Standard Deviation
Maximum Load (N)	10	0.4879	0.1394

Tensile Stress (MPa)	10	4.9847	6.5948
Young's Modulus (MPa)	10	59.9220	63.5329
Tensile Strain (mm/mm)	10	0.1743	0.039

Table 12: Tensile strength test for PBI with 0.5% GOFT

Data	N Total	Mean	Standard Deviation
Maximum Load (N)	10	0.375	0.164
Tensile Stress (MPa)	10	4.346	3.263
Young's Modulus (MPa)	10	74.871	68.314
Tensile Strain (mm/mm)	10	0.156	0.034

Table 13: Tensile strength tests for PBI with 1.0% GOFT

Data	N Total	Mean	Standard Deviation
Maximum Load (N)	10	0.4361	0.1418
Tensile Stress (MPa)	10	1.5023	0.5866
Young's Modulus (MPa)	10	15.9880	7.6409
Tensile Strain (mm/mm)	10	0.2014	0.0423

The next set of tensile testing data demonstrated the tensile behavior of PBI nanofibers with 0.1%, 0.5% and 1.0% (with respect of the polymer mass) GOFT (EG). Following the previous tensile testing result addition 0.1% GOFT (EG) decreased the Young's modulus and tensile

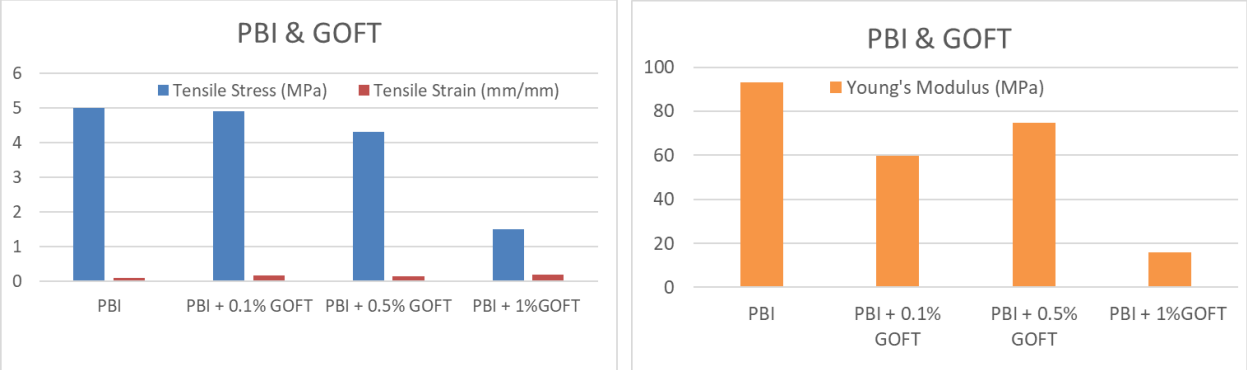

Figure 23: Tensile parameters for PBI nanofibers with GOFT

stress and increase tensile strain of PBI nanofiber. Addition of 0.5% of GOFT (EG) made more decrease in the Young's modulus and tensile stress and increase the tensile strain. But the highest percentage of GOFT (EG) offered a different observation, addition of 1.0% GOFT (EG) increased the Young's modulus, tensile stress and tensile strain of PBI nanofiber. PBI nanofiber with 1.0% GOFT (EG) is strong and tough with high resistivity of deformation and tensile strength.

Table 14: Tensile strength test for PBI with 0.1% GOFT (EG)

Data	N Total	Mean	Standard Deviation
Maximum Load (N)	10	0.4072	0.0938
Tensile Stress (MPa)	10	3.9120	3.2757

Young's Modulus (MPa)	10	55.0971	28.0554
Tensile Strain (mm/mm)	10	0.1315	0.0247

Table 15: Tensile strength tests for PBI with 0.5% GOFT (EG)

Data	N Total	Mean	Standard Deviation
Maximum Load (N)	10	0.308	0.126
Tensile Stress (MPa)	10	2.675	1.552
Young's Modulus (MPa)	10	40.808	25.062
Tensile Strain (mm/mm)	10	0.164	0.035

Table 16: Tensile strength tests for PBI with 1.0% GOFT (EG)

Data	N Total	Mean	Standard Deviation
Maximum Load (N)	10	1.2697	0.5961
Tensile Stress (MPa)	10	6.1841	3.0150
Young's Modulus (MPa)	10	138.8638	97.9509
Tensile Strain (mm/mm)	10	0.1423	0.0373

Some polymers have unique surface characteristics, this unique surface quality restricts evenly dispersion of graphene within polymer matrix and causes agglomeration of graphene. This agglomeration leads to the poor mechanical properties of polymer nanofiber.[2]

Table 17 demonstrated the numerical values of the tensile testing observation. From the

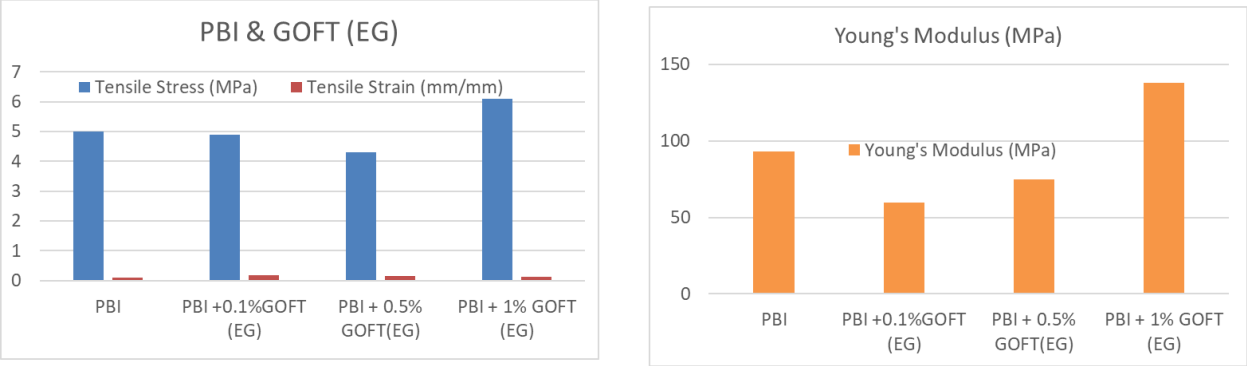

Figure 24: Tensile parameters for PBI nanofibers with GOFT (EG)

numerical value it was observed that the PEI nanofiber has low tensile stress and tensile stress is slightly higher than strain and there is low possibility of elongation. PEI has low Young's modulus about 5.9 MPa. According to the result PEI is not rigid and strong with low resistivity of deformation and tensile strength.

Table 17: Tensile strength tests for PEI

Data	N Total	Mean	Standard Deviation
Maximum Load (N)	10	1.2697	0.5961
Tensile Stress (MPa)	10	6.1841	3.0150

Young's Modulus (MPa)	10	138.8638	97.9509
Tensile Strain (mm/mm)	10	0.1423	0.0373

With the addition of reinforcing material EG, there was a slight decrease in Young's modulus, PEI nanofiber with 0.1 % EG has Young's modulus about 5.4 MPa with lower tensile strain and tensile stress. With the increase in percentage, PEI nanofiber with 0.5% EG experienced lower Young's modulus, tensile stress and higher tensile strain than 0.1%. PEI nanofiber with 1% EG also experience lower Young's modulus, tensile stress and higher tensile strain than 0.1% but Young's modulus and tensile stress value are higher than 0.5%.

This observation indicates that the addition of EG makes PEI nanofibers become flexible with lower resistivity of deformation.

Table 18: Tensile strength tests for PEI with 0.1% EG

Data	N Total	Mean	Standard Deviation
Maximum Load (N)	8	0.186	0.079
Tensile Stress (MPa)	8	0.497	0.167
Young's Modulus (MPa)	8	5.395	5.167
Tensile Strain (mm/mm)	8	0.266	0.117

Table 19: Tensile strength tests for PEI with 0.5% EG

Data	N Total	Mean	Standard Deviation
Maximum Load (N)	10	0.130	0.034
Tensile Stress (MPa)	10	0.362	0.098
Young's Modulus (MPa)	10	1.380	0.470
Tensile Strain (mm/mm)	10	0.447	0.121

Table 20: Tensile strength tests for PEI with 1.0% EG

Data	N Total	Mean	Standard Deviation
Maximum Load (N)	7	0.136	0.081
Tensile Stress (MPa)	7	0.613	0.388
Young's Modulus (MPa)	7	4.415	5.829
Tensile Strain (mm/mm)	7	0.327	0.096

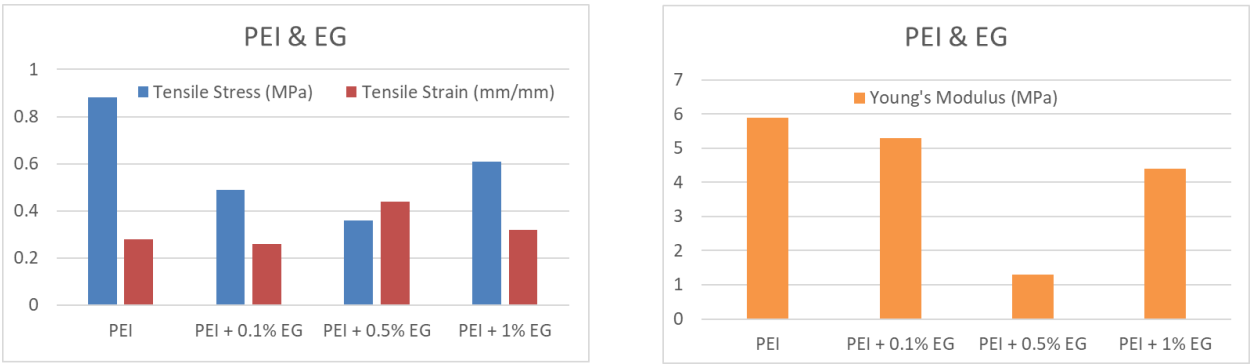

Figure 25: Tensile parameters for PEI nanofibers with EG

The next table demonstrated the tensile behavior of PEI nanofibers with 0.1%, 0.5% and 1.0% GOFT. With the addition of GOFT, PEI nanofibers experienced increase in Young's modulus and tensile stress value and decrease in tensile strain value. For nanofiber with 0.1% GOFT Young's modulus increased up to 9.9 MPa, the tensile stress was 2.9 MPa and tensile strain increased up to 0.29. With the increasing percentage of GOFT, PEI nanofiber with 0.5% GOFT there was decrease in Young's modulus, tensile stress and tensile strain value though the values were higher than the tensile parameters of PEI nanofiber without any reinforcing material. With highest percentage of GOFT PBI nanofiber experienced the highest young modulus and tensile stress among all the three percentages of GOFT, on the other hand it experienced the lowest tensile strain value. Observing all these tensile testing output, it can be concluded that the addition of GOFT increase the deformation rigidity and decrease the flexibility of PEI nanofiber and PEI nanofibers with GOFT are more rigid and strong than PEI nanofibers without GOFT.

Table 21: Tensile strength tests for PEI with 0.1% GOFT

Data	N Total	Mean	Standard Deviation
Maximum Load (N)	10	0.1439	0.0770
Tensile Stress (MPa)	10	2.9245	3.4095
Young's Modulus (MPa)	10	9.8077	4.0801
Tensile Strain (mm/mm)	10	0.2933	0.0726

Table 22: Tensile strength tests for PEI with 0.5% GOFT

Data	N Total	Mean	Standard Deviation
Maximum Load (N)	10	0.2021	0.0632
Tensile Stress (MPa)	10	0.8890	0.4605
Young's Modulus (MPa)	10	8.7784	3.9874
Tensile Strain (mm/mm)	10	0.2122	0.0462

Table 23: Tensile strength tests for PEI with 1.0% GOFT

Data	N Total	Mean	Standard Deviation
Maximum Load (N)	10	0.2627	0.0917
Tensile Stress (MPa)	10	1.1497	0.4997
Young's Modulus (MPa)	10	16.4471	16.4615
Tensile Strain (mm/mm)	10	0.2373	0.0819

The next set of tensile testing data demonstrated the tensile behavior of PEI nanofibers with 0.1%, 0.5% and 1.0% GOFT (EG). Addition of 0.1% GOFT (EG) decreased the Young's modulus and tensile stress and increase tensile strain of PEI nanofiber. Addition of 0.5% of GOFT (EG) made sharp increase in the Young's modulus and tensile stress and slight increase

the tensile strain.

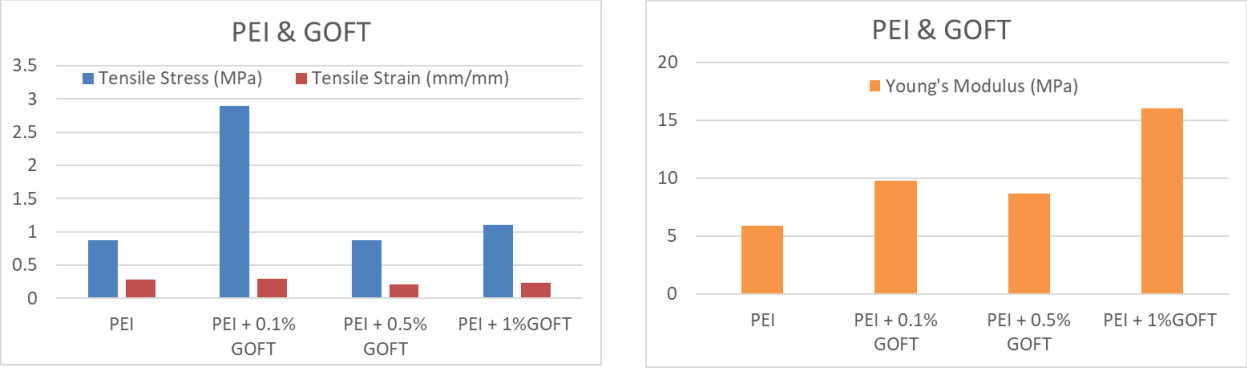

Figure 26: Tensile parameters for PEI nanofibers with GOFT

Addition of 1.0% GOFT (EG) also increased the young modulus, tensile stress and tensile strain of PEI nanofiber but these values were lower than the tensile parameters of PEI nanofiber with 0.5% GOFT (EG). PEI nanofibers with GOFT (EG) are strong and tough with high resistivity of deformation and tensile strength.

Table 24: Tensile strength test for PEI with 0.1% GOFT (EG)

Data	N Total	Mean	Standard Deviation
Maximum Load (N)	10	0.1769	0.0553
Tensile Stress (MPa)	10	0.9761	0.3908
Young's Modulus (MPa)	10	5.3887	3.3054
Tensile Strain (mm/mm)	10	0.3944	0.1223

Table 25: Tensile strength tests for PEI with 0.5% GOFT (EG)

Data	N Total	Mean	Standard Deviation
Maximum Load (N)	10	0.4308	0.1456
Tensile Stress (MPa)	10	2.5252	0.8378
Young's Modulus (MPa)	10	20.9825	10.0953
Tensile Strain (mm/mm)	10	0.3789	0.1306

Table 26: Tensile strength test for PEI with 1.0% GOFT (EG)

Data	N Total	Mean	Standard Deviation
Maximum Load (N)	10	0.1569	0.0340
Tensile Stress (MPa)	10	1.7443	1.7957
Young's Modulus (MPa)	10	6.7246	3.6392
Tensile Strain (mm/mm)	10	0.4145	0.1397

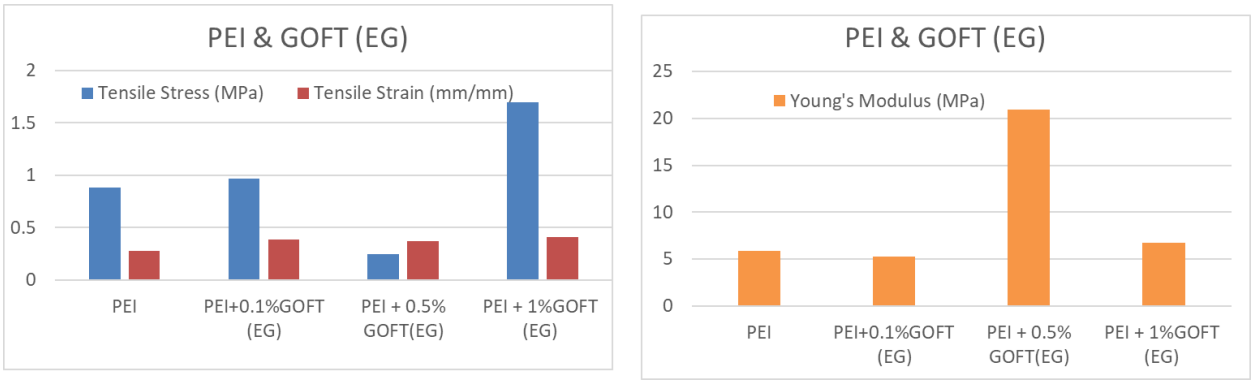

Figure 27: Tensile parameters for PEI nanofibers with GOFT (EG)

CHAPTER VII

THERMOPHYSICAL ANALYSIS

Introduction

TGA is a technique of thermal analysis used for the determination physical and chemical properties of materials. In this analysis either temperature works as a function where heating rate remains constant, or time works as a function by keeping the mass loss and temperature constant. Through this analysis physical properties like phase transition, vaporization desorption and chemical properties like decomposition, dehydration can be observed. For polymer TGA provides necessary information through mass loss or mass gain of polymer samples happen due to decomposition, degradation, oxidation, loss of volatile compound. Moreover, thermal stability of polymer material can be measured easily following TGA testing procedures by observing thermal decomposition or degradation.[25]

DSC is a thermo analytical technique where energy transformation is usually measured for a physical change or chemical change of a sample. In this technique a reference material is required to calculate the necessary energy change for the increase or decrease of the sample temperature. For polymer samples DSC provides necessary information related with oxidation stabilities, thermal degradation, and water loss. It also provides information for the determination of glass transition temperature of polymer.[25]

Instrument

A Perkin-Elmer TGA 7 instrument was used for thermogravimetric analysis. For differential scanning calorimetry (DSC) a Perkin-Elmer DSC 7 was used under nitrogen environment with maximum temperature 250 °C.

Method

TGA

Samples were placed in an oven at 70 ℃ for two hours to dry and to remove solvents and water. About 4-5 mg sample was placed on a sample pan and enclosed in the furnace. In this process sample decomposed in nitrogen gas environment. The flow rate was 20mL/min and temperature were about 20.0 ℃ initially. The final temperature was 600 ℃ and flow rate was 10.00℃/min.[25]

DSC

For DSC measurement two cells are required generally. One of them is for sample and another is used as reference. A small amount of sample (1-15 mg) is enough for DSC measurement. Usually, DSC experiments contained heating and cooling of the sample at particular steady rate and observed heat flow is used for characterizing the phase transition as a function of temperature. Experiments are carried out in nitrogen environment. Flow rate is kept around 20 ml/min. The total heating and cooling process kept paused in regular intervals for 1 to 15 min. Constant slow heating and cooling process provides well defined Tg value.[25]

Results and discussion

TGA

GOFT The degradation of PBI started from 100 °C and stopped at 700 °C.PBI nanofiber with 1% EG also had the similar degradation temperature range. From derivative weight vs temperature curve, it was observed that there was a prominent peak at 100°C, 300°C and 750°C. For PBI with 1% EG sample, no significant changes were observed compared to PBI, but around 446 °C there was a peak like appearance. As no significant difference was observed in degradation temperature range, it could be interpreted that the addition of 1% EG did not significantly change thermal stability of PEI nanofiber.

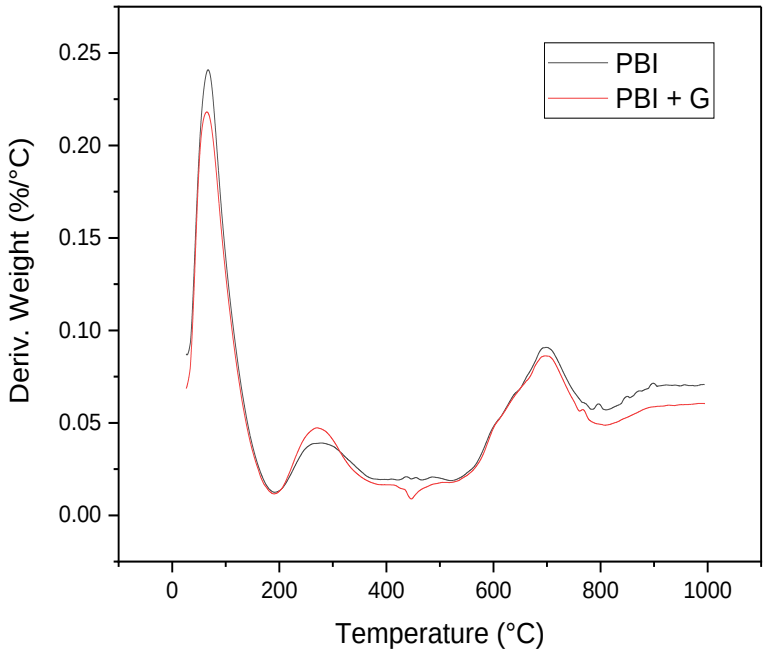

Figure 28: Derivative thermogravimetric curves of PBI

On the other hand, the degradation of PEI started at 400 °C and stopped at 650 °C.PEI nanofiber with 1% EG also had the similar degradation temperature range. From derivative

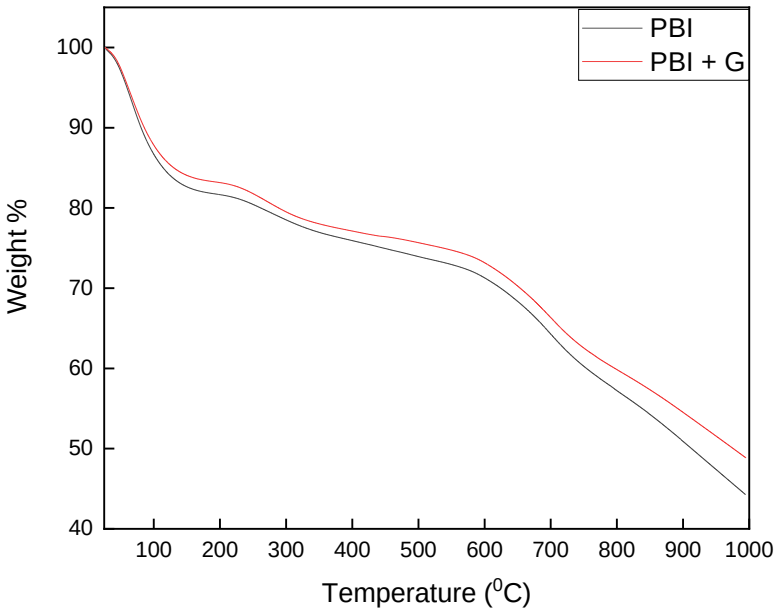

Figure 29: Mass loss Vs temperature thermograms of PBI

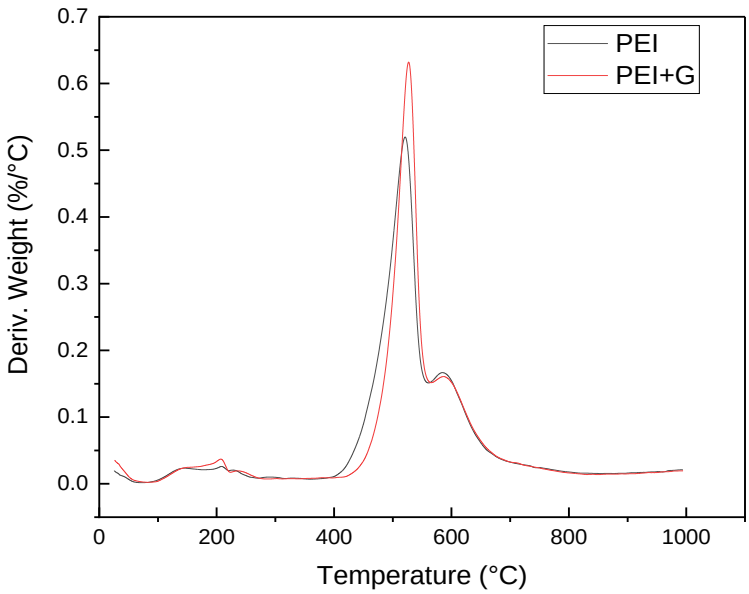

Figure 30: Derivative thermogravimetric curves of PEI

weight vs temperature curve it was observed that there was a prominent peak at 520°C and 600°C. For PEI with 1% EG sample, no significant changes were observed compared to PEI. As no significant difference was observed in degradation temperature range, it can be

interpreted that the addition of 1% EG did not significantly change the thermal behavior of PEI nanofiber.

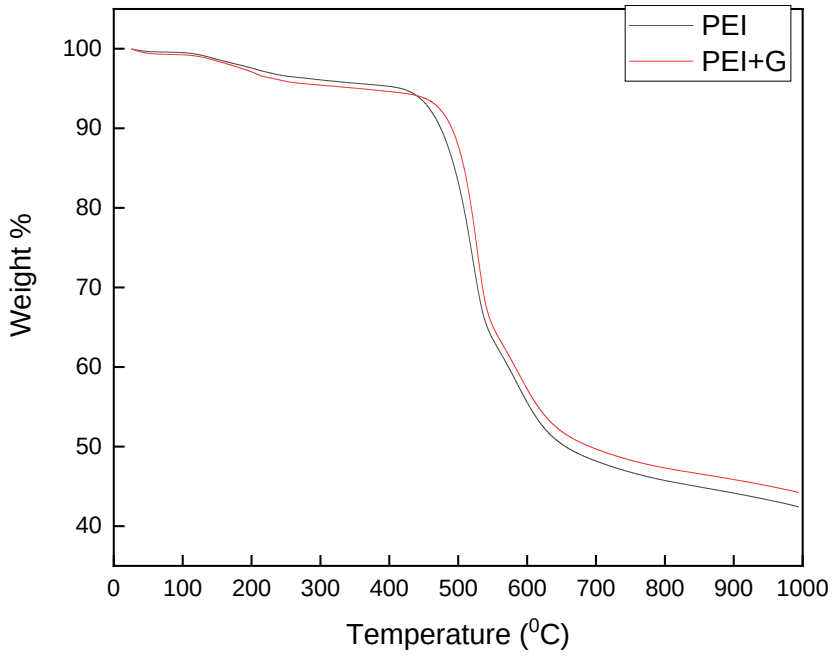

Figure 31: Mass loss Vs temperature thermograms of PEI

DSC

From the DSC thermogram of PBI and PBI + 1% EG it was observed that the Tg value of PBI was 95 ^{0}C and it had moved to 120 ^{0}C for PBI with 1% EG. With the addition of graphene filler, the Tg value increased up to 25 ^{0}C. For PEI and PEI with 1% EG the Tg value moved from 52 ^{0}C to 72 ^{0}C. The difference between the Tg value of PEI and PEI with graphene filler was about 20 ^{0}C. Tg value difference indicated weak physical interaction between polymer and graphene filler. The Tg value shifted to higher value with the addition of graphene reinforce material because Tg value is related with the mobility of polymer chain, presence of graphene filler restricts the mobility of polymer chain and results in higher Tg value.[25]

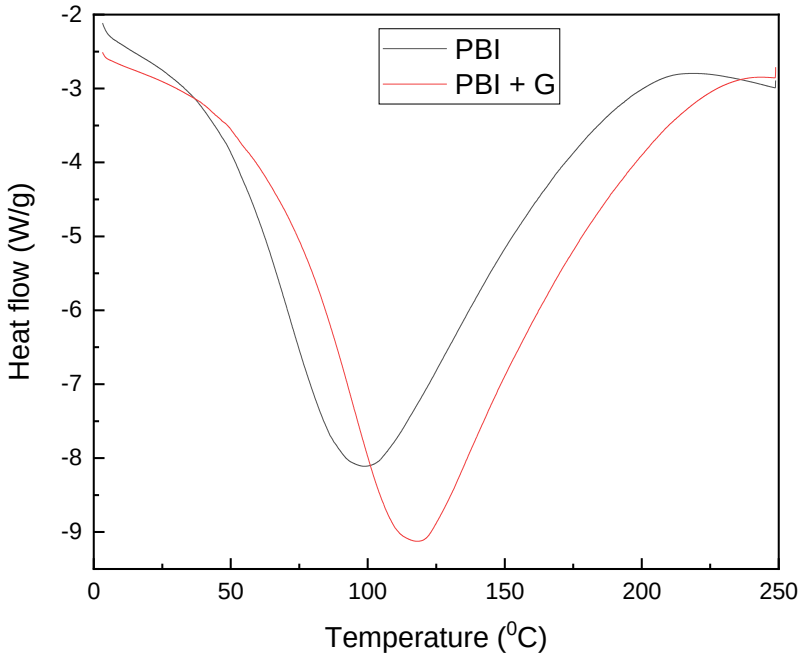

Figure 32: DSC thermograms of PBI and PBI + 1% EG

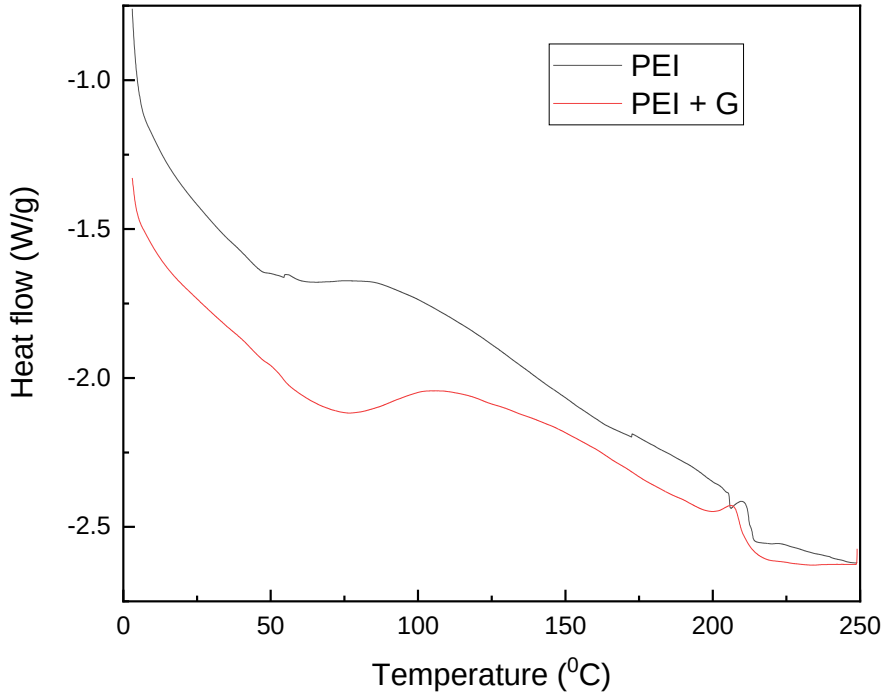

Figure 33: DSC thermograms of PEI and PEI + 1% EG

CHAPTER VIII

CONCLUSION

Graphene-based reinforce materials were synthesized successfully using simple and convenient method. Exfoliation of reinforcing material EG was confirmed using XRD and SEM.

Electrospun PBI and PEI polymer composite with three different of graphene-based reinforcing materials were prepared and characterized successfully.

Microscopic characterization was observed based on SEM technique. SEM micrograph of PBI nanofibers with 0.1% , 0.5% , 1.0 %(with respect to the polymer mass) of three graphene-based filler came up with no bead and experienced significant decrease in fiber diameter. This decrease was prominent in smaller amount of graphene loading while at higher percentage loading experienced a larger diameter. SEM micrographs of PEI nanofibers with these three graphene-based nanofiller also had flawless surface with no bead. With filler material EG PEI nanofibers experienced a significant increase in its diameter. But the addition of GOFT and GOFT (EG) decreased the fiber diameter. For PEI composite nanofibers narrow fiber diameter was obtained with the increasing percentage of filler material.

Spectroscopic characterization was done by FTIR-ATR spectroscopy. Based on the observation, there was almost negligible amount of change in characteristic functional group frequencies. Observation on the FTIR spectra provided the confirmation of no chemical disruption in the chemical structure of polymer with the addition of graphene filler. This also indicated weak

chemical structure of polymer with the addition of graphene filler. This also indicated weak physical interaction between polymer and filler materials.

By analyzing tensile testing results, it was observed that there was significant degradation in mechanical properties of PBI nanofibers with all three reinforcing materials. Only the PBI nanofiber with 1.0 % GOFT (EG) exhibited remarkable enhancement. On the other hand, PEI nanofibers with higher percent (0.5%, 1.0%) GOFT and GOFT (EG) achieved improved tensile strength. Best improvement was observed with 0.5% GOFT and 1% GOFT (EG). PBI and PEI nanofibers with EG had inferior mechanical properties.

Thermal characterization technique TGA confirmed that the thermal stability of PBI and PEI nanofibers was not disturbed by the addition of graphene nanofillers. There was no remarkable increase or decrease on the TGA results. It also indicated the fact of having weak physical interaction between polymer and graphene fillers.

Analyzing the Characterization results it can be interpreted that GOFT (EG) blended well into PBI matrix and GOFT dispersed almost homogeneously within PEI matrix. EG filler decreased the rigidity of both PBI and PEI.

According to the obtained characterization results, it was observed that a good combination of graphene filler and polymer depended on the nature of the polymer, nature of the graphene filler and homogeneous distribution of filler material within the polymer matrix. Surface nature and structure of PEI and PBI were different so the functional group interaction between graphene filler and polymer chain were also different. Obtaining homogeneous distribution of filler material within the polymer matrix is an essential pre-requirement and it mostly depends on the good dispersion and it was hard to achieve with these combinations

Effective exfoliation depends on the separation of the graphene layers with maximum space in the surface area gives polymer chain the maximum possibility to intercalate effectively. GOFT and GOFT (EG) exfoliated more potentially than EG and facilitated PEI and PBI nanofibers with improved properties.

REFERENCES

1. Okpala C. Chikwendu. “Nanocomposites – An Overview”. *International Journal of Engineering Research and Development* 11(2013): 17-23. Print

2. Mittal, Vikas. “Functional Polymer Nanocomposites with Graphene: A Review”. *Macromolecular Material and Engineering* 299(2014): 906-931.Print

3. Avila-Vega, I. Yazmin, Leyva-Porras, C. Cesar, Mireles Marcela, Quevedo- Lopez Manuel, Macossay Javier and Bonilla-Cruz Jose. “Nitroxide-Functionalized Graphene Oxide from Graphite Oxide”. *Carbon* 63(2013): 376-389. Print

4. Ding Yichun, Hou Haoqing, Zhao Yong, Zhu Zhengtao and Fong Hao. “Electospun Polyimide Nanofibers and their Applications”. *Progress in polymer science* 61(2016): 67-103. Print

5. Anandan S., Ponprapakaran K. and Sentheil T. “Parametric Study of Manufacturing Ultrafine Polybenzimidazole Fibers by Electrospinning”. *International Journal of Plastic Technology* 10(2012): 12588-12603.Print

6. Chee W. K., Lim H.N., Huang N. M. and Harrison I. “Nanocomposite of Graphene/Polymer: A review”. *RSC Advanced* 5(2015): 68014-68051.Print

7. Macossay Javier, Sheikh A. Faheem, Cantu Travis, Embanks M. Tom, Salinas M. Esther, Farhangi S. Chakavak, Ahmed Hassan, Hassan M. Shamshi, Khil S. Myung, Maffi K. Shivani, Kim Hern and Bowlin I. Gary. “Imaging, Spectroscopic, Mechanical and Biocompatibility Studies of Electrospun Tacoflex ^{R} EG 80 A Nanofibers and Composites Thereof Containing Multiwalled Carbon Nanotubes”. *Applied surface science* 321(2014): 205-213. Print

8. Leyva-Porras, C. Cesar, Gutierrez C. Ornelas, Yoshida M. Miki, Avila-Vega, I. Yazmin, Macossay Javier and Bonilla-Cruz Jose. “EELS Analysis of Nylon 6 Nanofibers Reinforced with Nitroxide-Functionalized graphene Oxide”. *Carbon* 70(2014): 164-171.Print

9. Macossay Javier, Ana V. R. Ybarra, Faheem A. Arjamend, Cantu travis, Embanks M. Tom, Chipara Mircea, Lopez C. Enrique and Noriega M Nasser. “Electrospun Polystyrene- multiwalled Carbon Nanotubes: Imaging, Thermal and Spectroscopic Characterization”. *Designed Monomers and Polymers* 15(2012): 197-205. Print

10. Macossay Javier, Leal H. Juan, Kuang Anxiu and Jones E. Robert. “Electrospun Fibers from Poly(Methyl methacrylate)/ Vapor Grown Carbon Nanofibers”. *Polymers for advanced technologies* 17(2006): 391-394. Print

11. Dawkins B.G., Qin F., Gruender M. and Copeland G. S. “Polybenzimidazole (PBI) High Temperature Polymers and Blends”. *High temperature polymer blend* 7(2014):174-212.Print

12. Obregon Nancy, Agubra Victor, Pokhrel Madhab, Campos Howard, Flores David, De la Garza, Mao Yuanbing, Macossay Javier and Alcoutlabi Mataz. “Effect of Polymer Concentration, Rotational Speed and Solvent Mixture on Fiber Formation using Forcespinning”. *Fibers* 4(2016):20-35. Print

13. Macossay Javier, Marruffo Alexis, Salinas Samuel and Lozano Karen. “Thermal Studies and Physical Structure of Poly (Methyl methacrylate)/ Vapor Grown Carbon Nanofibers Composites Prepared Through In Situ Bulk Polymerization”. *Journal of Undergraduate Chemistry Research* 1(2007): 23-28. Print

14. Padron Maggie and Macossay Javier. “Investigation of the Parameters for Electrospinning of PBI in DMAc”. *Report for Chem problem* 2019.Print

15. Macossay Javier, Avila-Vega, I. Yazmin, Sheikh A. Faheem, Cantu Travis, Rodriguez E.L. Francisco, Soria H. R. Edgar, Advincula C. Rigoberto and Bonilla-Cruz Jose. “The Role of Alpha, Gamma and Metastable Polymorphs on Electrospun Polyimide 6/Functionalized Graphene Oxide”. *Macromolecular rapid communication* 10 (2020): 2000195-2000200. Print

16. Garcia Ivan and Macossay Javier. “Graphene Exfoliation via Microwave Irradiation”. *Report for Chem problem* 2019.Print

17. B. C. Paul, G. Arthi and B.D. Lignesh. “A Simple Approach to Stepwise Synthesis of Graphene Oxide Nanomaterial”. *Journal of Nanomedicine and Nanothechnology 6* (2015):253-258. Print

18. Ahmed Mausa, Gert Heinrich, Udo Wagenknecht and Omar Arabeyat. “The Efffect of Exfoliated Graphite on the Thrmal and Mechanical Properties of Dynamically Vulcanized Polystyrene/Styrene Butadiene Rubber Composite”. *Journal of engineering materials and technology* 140 (2018):11002-11007. Print

19. Wei Tong, Fan Zhuangjun, Luo Guilian, Zheng Chao and Xie Dashou. “A Rapid and Effient Method to Prepare Exfoliated Graphite by Micreowave Irradiation”. *Carbon* 47(2008): 337-339. Print

20. Bang S. Gyeong, So M. Hye, Lee J. Min and Ahn W. Chi. “Preparation of graphene with Few Defects using Eapanded Graphite and Rose Bengal”. *Journal of Material chemistry* 22(2012): 4806-4810. Print

21. Dimiev M. Ayrat and Tour M. James. “Mechanism of Graphene Oxide Formation”. *ACS Nano* 8(2014): 3060-3068. Print

22. Li Wei, Han Chong, Liu Wei, Zhang Minghui and Tao Keyi. “Expanded Graphite Applied in the Catalytic Process as a catalyst Support”. *Catalysis Today* 125(2007): 278-281. Print

23. Bradbury Salvi. “Scanning Electron Microscope”. *Britannica (Instrument)*. Elctronic

24. Oberon Nancy and Macossay Javier. Microwave-assisted Ring-opening Polymerization Of Poly(ϵ-Caprolactone). *Thesis manuscript for Master’s* (2018). Print

25. Ybarra V. R. Ana and Macossay Javier. “Electrospun Polystyrene- multiwalled Carbon Nanotubes: Imaging, Thermal and Spectroscopic Characterization”. *Thesis manuscript for Master’s* (2012). Print

26. Anderson J. M. and Voskerician G. “The challenge of biocompatibility evaluation of biocomposites”. *Biomedical composites* (2010): Chapter14. Print

BIOGRAPHICAL SKETCH

Fatema Ha-mim was born in Rangpur, Bangladesh in 1991.She received her Bachelor's in Chemistry from University of Dhaka, Bangladesh in 2013 and her first Master's in Chemistry from University of Dhaka in 2015. Her main research interest is to synthesis graphene based nanofiller and electrospinning. After earning her MS in Chemistry from the University of Texas Rio Grande Valley in 2021, she is looking forward to enrolling on PhD program in United States.

Permanent address: House No 235 Road No 02 Circuit house lane Dhap Rangpur-5400, Bangladesh.

Permanent email address: fatema.hamim@gmail.com